

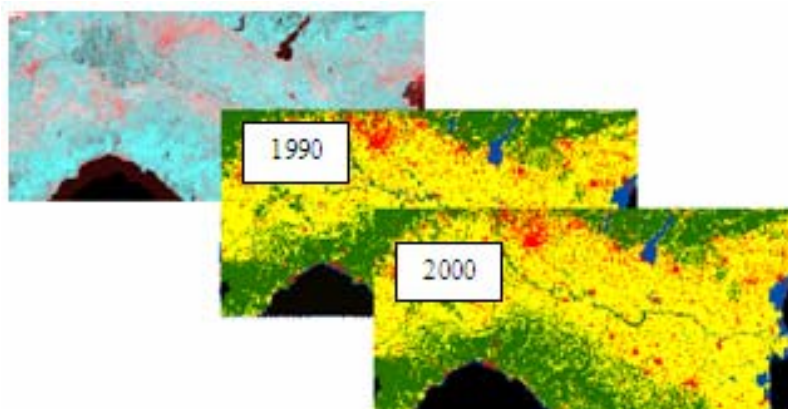
Centre for Geo-Information

Thesis Report GIRS-2006-23

LAND COVER MONITORING BY MEANS OF MEDIUM RESOLUTION SATELLITE IMAGERY

- a Case Study in Northern Italy -

Petra D'Odorico



April / 2006



WAGENINGEN UNIVERSITY
WAGENINGEN UR

LAND COVER MONITORING BY MEANS OF MEDIUM RESOLUTION SATELLITE IMAGERY

- a Case Study in Northern Italy -

Petra D'Odorico

Registration number 82 08 03 167 080

Supervisors:

Ir. Caspar A. Mücher

Prof. Dr. sc. nat. Michael E. Schaepman

A thesis submitted in partial fulfilment of the degree of Master of Science at
Wageningen University and Research Centre, The Netherlands.

April, 2006
Wageningen, The Netherlands

Thesis code number: GRS-80436
Wageningen University and Research Centre
Laboratory of Geo-Information Science and Remote Sensing
Thesis Report: GIRS-2006-23

Acknowledgements

I hereby express my most sincere gratitude to my supervisors Ir. Sander Mücher and Prof. Dr. Michael Schaepman for their guidance and precious advice throughout the course of my thesis work. I particularly thank them for having stimulated my interest for Remote Sensing and its applications such as land cover mapping and monitoring.

Next, I would like to extend my appreciation to all MGI and Alterra staff members for the marvellous and motivating working-environment they have contributed to create. Particularly, I want to thank Ing. Willy ten Haaf for his valuable guidance as student advisor. I am moreover grateful to Ing. Aldo Bergsma, Drs. Harm Bartholomeus and Raul Zurita Milla for sharing interesting discussions on relevant issues of my thesis work and for their advice. Many thanks go also to Drs. Allard de Wit for his availability in solving critical technical constraints.

I want to express my deepest affection to all my MGI colleagues and friends for making this time so special and enriching me as a person. Above all, I like to express my most sincere thanks to Alemu for his irreplaceable presence day in and day out, for all the patience, support and encouragement, for having added such joy and love to my days.

Last but not least, my heart felt thanks goes to my family and especially to my parents Anna and Sandro D'Odorico for their understanding, love and constant support.

Abstract

Nowadays many of the environmental policy coming from the European Union are based on the outcome of environmental models, whose primary input are data on land cover and land use. Particularly, an increasing desire to monitor dynamics of the urban land cover is being observed in the scientific community. This tendency can be attributed to the recognition of urbanization phenomena as one of the key pressures on biodiversity as delineated in the BIOPRESS initiative.

This study attempts to evaluate the utility of medium spatial resolution satellite data for land cover mapping and monitoring in the spatial-temporal dimension. The chosen product is the daily Terra/MODerate resolution Imaging Spectroradiometer (MODIS) atmospherically corrected surface reflectance product at 250m resolution (MOD09GQK). Its potential was evaluated in the context of the Co-ordination of Information on the Environment (CORINE) land cover database-update effort and focuses on the classes defined in CORINE's first Nomenclature Level, namely artificial surfaces (urban), agricultural areas, forested areas and water/wetlands. A case study was performed in the northern part of the Italian peninsula, in the so called Po' valley. Land cover changes affecting the urban class in this area were of particular interest for the present study.

A series of semi-automatized procedures were developed for MODIS data pre-processing, 1990 simulation, as well as training and execution of Maximum Likelihood classifications. Simulation was performed through linear regression analysis attempting to model the relationship between MODIS and Landsat data. The MODIS 2000 classification was performed for a single-date and for a multitemporal dataset, eventually results were compared. CORINE's land cover maps were used as 'ground truth' for the validation of the MODIS classifications, a comparison between a pixel- and an object-wise assessment was carried out. Eventually, a post-classification change detection method was applied to derive change signals occurring in the 1990-2000 time interval.

The methodology adopted in this study showed to be successful in proving the potential of 250m resolution MODIS data for land cover mapping and monitoring on the regional scale. Classification accuracies showed good agreement with CORINE land cover maps, ranging from kappa values of 0.59 to 0.88. The change detection results confirmed the suitability of this MODIS product as an alarm product identifying areas where significant land cover conversion has been taken place and should be investigated further by means of higher resolution data. Nevertheless, they also suggested the shortage of the same product for areal estimation of land cover changes. In general, the urban land cover class showed itself as a problematic class due to the small size and scattered distribution of its elements and to the absence of a clear "spectral urban signal". Classification results revealed how this class is underestimated as a consequence of the coarsening of the resolution leading to ambiguity in the change figures.

Keywords: *Land cover/use change; Urbanization; Land cover mapping and monitoring; Medium resolution satellite data; MODIS; CORINE; Post-classification change detection.*

Table of Contents

| | |
|---|-------------|
| <u>ACKNOWLEDGEMENTS</u> | <u>III</u> |
| <u>ABSTRACT</u> | <u>IV</u> |
| <u>TABLE OF CONTENTS</u> | <u>V</u> |
| <u>LIST OF TABLES</u> | <u>VII</u> |
| <u>LIST OF FIGURES</u> | <u>VIII</u> |
| <u>ABBREVIATIONS AND ACRONYMS</u> | <u>IX</u> |
| <u>SYMBOLS AND PARAMETERS</u> | <u>X</u> |
| <u>1. INTRODUCTION</u> | <u>1</u> |
| 1.1. BACKGROUND | 1 |
| 1.2. PROBLEM DEFINITION | 2 |
| 1.3. RESEARCH OBJECTIVES | 4 |
| 1.5. RESEARCH HYPOTHESIS | 5 |
| 1.6. REPORT STRUCTURE | 6 |
| <u>2. LITERATURE REVIEW</u> | <u>7</u> |
| 2.1. LAND COVER MONITORING AND REMOTE SENSING | 7 |
| 2.1.1 LAND COVER/USE CHANGE | 7 |
| 2.1.2. INSTRUMENT PROPERTIES INFLUENCING LAND COVER MAPPING | 9 |
| 2.1.3. MAPPING OF URBAN LAND COVER | 10 |
| 2.2. MEDIUM RESOLUTION SATELLITES: MODIS | 13 |
| 2.3. CHANGE DETECTION TECHNIQUES | 16 |
| <u>3. MATERIALS AND METHODS</u> | <u>19</u> |
| 3.1. STUDY AREA AND TIME INTERVAL | 19 |
| 3.2. DATA | 20 |
| 3.2.1. REMOTE SENSING DATA | 20 |
| 3.2.2. LAND COVER DATASETS | 23 |
| 3.3. METHODOLOGICAL CONCEPTUAL MODEL | 24 |
| 3.4. PREPROCESSING | 26 |
| 3.4.1. MODIS | 26 |
| 3.4.2. LANDSAT | 26 |
| 3.4.3. CORINE | 30 |
| 3.4.4. DATASETS CO-REGISTRATION | 32 |
| 3.5. SIMULATION MODIS 1990 | 34 |
| 3.6. CLASSIFICATION | 37 |

| | |
|---|-----------|
| 3.6.1. UNSUPERVISED CLASSIFICATION MODIS 2000 | 38 |
| 3.6.2. SUPERVISED CLASSIFICATION MODIS 2000: SINGLE DATE VERSUS MULTITEMPORAL APPROACH | 39 |
| 3.6.3. SUPERVISED CLASSIFICATION SIMULATED MODIS 1990 | 41 |
| 3.7. ACCURACY ASSESSMENT | 41 |
| 3.7.1. PIXEL BASED VALIDATION | 42 |
| 3.7.2. OBJECT BASED VALIDATION | 44 |
| 3.8. CHANGE DETECTION | 45 |
| 4. RESULTS AND DISCUSSION | 47 |
| 4.1. SIMULATION MODIS 1990 | 47 |
| 4.2. CLASSIFICATION | 49 |
| 4.2.1. UNSUPERVISED CLASSIFICATION MODIS 2000 | 49 |
| 4.2.2. SUPERVISED CLASSIFICATION MODIS 2000 | 53 |
| 4.2.2.1. Validation of pixel-wise results | 53 |
| 4.2.2.2. Validation of object-wise result | 61 |
| 4.2.3. SUPERVISED CLASSIFICATION MODIS 1990 | 65 |
| 4.3. CHANGE DETECTION | 69 |
| 4.3.1. TIME ONE IMAGE: SIMULATED MODIS 1990 CLASSIFICATION | 69 |
| 4.3.2. TIME ONE IMAGE: CLC1990 DATASET | 71 |
| 4.3.2.1. Pixel-wise approach | 71 |
| 4.3.2.2. Object-wise approach | 73 |
| 5. CONCLUSIONS AND RECOMMENDATIONS | 77 |
| 5.1. CONCLUSIONS | 77 |
| 5.2. RECOMMENDATIONS | 79 |
| BIBLIOGRAPHY | 81 |
| APPENDIX | 88 |

List of Tables

| | |
|--|----|
| Table 1 Terra/MODIS surface reflectance product characteristics..... | 21 |
| Table 2 Landsat TM and ETM+ scene specific acquisition dates | 22 |
| Table 3 The CORINE land cover project in figures (source: CORINE land cover Technical Guide, Bossard <i>et al.</i> , 2000)..... | 24 |
| Table 4 Registration settings for Landsat TM, MODIS and ETM scenes..... | 33 |
| Table 5 Class Training Sample separability (Transformed Divergence)..... | 40 |
| Table 6 Regression models for MODIS 1990 simulation..... | 47 |
| Table 7 Confusion matrix MODIS 2000 multitemporal dataset using K-Means unsupervised approach versus CLC2000 ‘ground truth’ | 51 |
| Table 8 Confusion matrix MODIS 2000 single-date (June) using Maximum Likelihood classification algorithm versus CLC2000 ‘ground truth’ | 58 |
| Table 9 Confusion matrix MODIS 2000 multitemporal using Maximum Likelihood classification algorithm versus CLC2000 ‘ground truth’ | 59 |
| Table 10 Confusion matrix ‘object-based’ MODIS 2000 multitemporal classification versus CLC2000 ‘ground truth’ | 63 |
| Table 11 Confusion matrix MODIS 1990 simulated using Maximum Likelihood classification algorithm versus CLC1990 ‘ground truth’ | 67 |
| Table 12 Change Report for unitemporal approach (time one image: simulated MODIS 1990 classification; time two image: original MODIS 2000 classification) | 70 |
| Table 13 Change Report for multitemporal approach (date one image: CLC1990 classification; date two image: MODIS 2000 multitemporal classification)..... | 71 |
| Table 14 Change Report for multitemporal approach (date one image: CLC1990 classification; date two image: ‘object-based’ MODIS 2000 multitemporal classification) | 73 |

List of Figures

| | |
|--|----|
| Figure 1 Location of the study area, north Italy..... | 20 |
| Figure 2 Flow chart of working scheme | 25 |
| Figure 3 CORINE land cover classification images after recoding to 4 thematic classes (level 1 CLC Nomenclature). (A) 1990, and (B) 2000..... | 31 |
| Figure 4 Classification image MODIS 2000 multitemporal dataset using K-Means unsupervised approach..... | 50 |
| Figure 5 Classification image MODIS 2000 single-date (June) dataset using Maximum Likelihood classification algorithm..... | 57 |
| Figure 6 Classification image MODIS 2000 multitemporal dataset using Maximum Likelihood classification algorithm | 57 |
| Figure 7 Classification image MODIS 2000 multitemporal dataset resampled to CORINE's polygon level by means of zonal majority rule..... | 62 |
| Figure 8 Classification image MODIS 1990 simulated dataset using Maximum Likelihood classification algorithm | 66 |
| Figure 9 Urban centres, for which a comparison between the pixel- and the object- level change identification, has been performed..... | 75 |
| Figure 10 Sample of urban centres located within the study area. Satellite image: MODIS 2000 dataset displayed in red-NIR-NIR layer combination. Left hand side: pixel-level results; Right hand side: object-level results..... | 76 |

Abbreviations and Acronyms

| | |
|--------|---|
| AVHRR | Very High Resolution Radiometer |
| CLC | CORINE Land Cover |
| CORINE | Co-ordination of Information on the Environment |
| DB | Data Base |
| DCW | Digital Chart of the World |
| DIS | Data and Information System |
| DN | Digital Number |
| EEA | European Environmental Agency |
| EMS | Electro Magnetic Spectrum |
| ENVI | Environmental for the Visualization of Images |
| EOS | Earth Observing System |
| ETM | Enhance Thematic Mapper |
| GCP | Ground Control Points |
| GLCF | Global Land Cover Facility |
| GMES | Global Monitoring for the Environment and Security ¹ |
| IDL | Interactive Data Language |
| IGBP | International Geosphere-Biosphere Programme |
| JRC | Joint Research Centre |
| MERIS | Medium Resolution Imaging Spectrometer |
| ML | Maximum Likelihood |
| MODIS | MODerate resolution Imaging Spectroradiometer |
| MRT | MODIS Reprojection Tool |
| MSS | Multispectral scanner |
| NASA | National Aeronautics and Space Administration |
| NDVI | Normalized Difference Vegetation Index |
| NIR | Near InfraRed |
| NOAA | National Oceanic and Atmospheric Administration Advanced |
| PCA | Principal Component Analysis |
| PELCOM | Pan-European Land Cover Monitoring |
| RMSE | Root Mean Square Error |
| RTM | Radiative Transfer Model |
| SPOT | Satellite Pour l'Observation de la Terre |
| TD | Transformed Divergence |
| TM | Thematic Mapper |
| TOA | Top Of Atmosphere |
| USGS | United State Geological Survey |
| UTM | Universal Transverse Mercator |
| VCC | Vegetative Cover Conversion |
| WGS | World Geodetic System |

Symbols and Parameters

| | |
|--------------------------|--|
| L_{λ} | spectral radiance at the sensor's aperture in watts/(meter squared * ster * μm) |
| <i>GAIN</i> | rescaled gain (the data product "gain" contained in the Level 1 product header or ancillary data record) in watts/(meter squared * ster * μm) |
| <i>OFFSET</i> | rescaled bias (the data product "offset" contained in the Level 1 product header or ancillary data record) in watts/(meter squared * ster * μm) |
| <i>QCAL</i> | the quantized calibrated pixel value in DN |
| <i>LMIN</i> $_{\lambda}$ | the spectral radiance that is scaled to QCALMIN in watts/(meter squared * ster * μm) |
| <i>LMAX</i> $_{\lambda}$ | the spectral radiance that is scaled to QCALMAX in watts/(meter squared * ster * μm) |
| <i>QCALMIN</i> | the minimum quantized calibrated pixel value (corresponding to $\text{LMIN}\lambda$) in DN = 1 (LPGS Products) = 0 (NLAPS Products) |
| <i>QCALMAX</i> | the maximum quantized calibrated pixel value (corresponding to $\text{LMAX}\lambda$) in DN = 255 |
| ρ_{ρ} | unit less planetary reflectance |
| L_{λ} | spectral radiance at the sensor's aperture |
| d | earth-sun distance in astronomical units |
| <i>ESUN</i> $_{\lambda}$ | mean solar exoatmospheric irradiances |
| θ_s | solar zenith angle in degrees. |

1. Introduction

1.1. *Background*

Nowadays many of the environmental policy coming from the European Union are based on the outcome of environmental models, whose primary input are data on land cover and land use (Mücher *et al.*, 2000). Several have been the efforts made to exploit remotely sensed data for the purpose of land cover mapping of the European continent. Some of these efforts have focused on specific land cover classes such as forest cover, whereas few important activities have encompassed a wider purpose. Among the latter ones worth mentioning is the Co-ordination of Information on the Environment (CORINE) program started in 1985 from the European Union and now under supervision of the European Environmental Agency (EEA). This monitoring program is based on the collection and computer-assisted visual interpretation of high resolution satellite images e.g. Landsat Thematic Mapper (TM) and SPOT HRV data, at a scale of 1:100 000, with support of ancillary data. The resulting land cover database (CORINE DB) distinguished between 44 classes grouped in a hierarchical scheme at three levels. CORINE's first version is dating 1990 whereas its update took place in 2000 (Boer *et al.*, 2000; Mücher *et al.*, 2000). A new update of CORINE land cover DB is being planned for next year based on satellite images of 2005 (Personal communication C.A. Mücher, 2006). Notwithstanding the accomplishment of the project which makes CORINE the most detailed database covering a large part of Europe (Mücher *et al.*, 2000), many are the challenges still present. It shortly became clear how a monitoring system relying almost exclusively on high resolution images is not sustainable in the long run. The small scene size of these images, which consequently means a significant data volume if all of Europe has to be covered, makes updates a time consuming and expensive task which can not be repeated with the desired frequency (Boer *et al.*, 2000). Moreover, the dissimilar conditions and preparations of the different countries involved, lead to different product qualities and product termination dates complicating the integration. Last but not least, the delineation of some of CORINE's classes has been strongly supported by ancillary data which introduce dependence and subjectivity with consequences for the updating (Mücher *et al.*, 2000).

A number of studies exists which have alternatively proposed the exploitation of the rich temporal information contained in the sequence of freely available coarse resolution satellite data (Jonathan *et al.*, 2005). The majority of those are based on data originating from the Advanced Very High Resolution Radiometer (AVHRR) onboard the US National Oceanic and Atmospheric Administration's (NOAA) polar orbiting satellite series. In 1992 the International Geosphere-Biosphere Programme for Data and Information System (IGBP-DIS) engaged in a monitoring program aiming at producing a global land cover set at a spatial resolution of 1 Km based on monthly NDVI maximum value composites. The limiting factor in this study was the absence of a stratification of the radiance data, recommended when dealing with heterogeneous and fragmented land cover. Moreover, the coarse spatial resolution of the dataset resulted in the definition of complex classes whose definition is difficult to apply (Mücher *et al.*, 2000). A further study exploiting AVHRR-NOAA 1.1 km resolution data is the Pan-European Land Cover Monitoring (PELCOM) program started in 1996 within the framework of the European Union. Differently from the previous approach in this study both multi-temporal NDVI profiles and multi-spectral AVHRR scenes have been input to the classification, thus exploiting the information content of both data characteristics. Unfortunately, the often small and fragmented changes typical of the European landscape combined with the limited geometric accuracy and low spatial resolution of NOAA-AVHRR images did not provide satisfying accuracies. Previous studies have shown how the classification accuracy does not reach the 70 % target, primary reasons being mixed pixel effects and the loss of small changes at sub-pixel level of AVHRR data (Boer *et al.*, 2000; Mücher *et al.*, 2000).

1.2. Problem Definition

The gap between the unaffordable time and cost investments of high resolution Landsat and SPOT images and the insufficient spatial properties of low resolution NOAA/AVHRR images are urging the land monitoring community to reach for alternative solutions. As aforementioned coarse resolution approaches have traditionally relied on data from NOAA's AVHRR sensor (1.1 Km) and it is only recently that data from NASA's MODerate resolution Imaging Spectroradiometer

(MODIS) sensor is been adopted for land cover/use monitoring activities. MODIS data feature better spatial resolution (up to 250m) and enhanced standards of calibration, georeferencing and atmospheric correction, as well as detailed per-pixel data quality information (Jonathan *et al.*, 2005).

The solution investigated with the present study is the possibility to use medium resolution sensors for land cover monitoring and specifically for urban growth mapping. MODIS 250m reflectance data were selected to test this hypothesis. MODIS data preserve the advantages offered by coarse resolution data, namely high temporal frequency, extensive coverage, and extremely low costs for data acquisition (Jonathan *et al.*, 2005), without at the same time having to lower excessively the spatial accuracy. Several authors have already successfully investigated the potential of MODIS data in the field of land cover mapping and change detection (Zhan *et al.*, 2000; Hansen *et al.*, 2002; Herold *et al.*, 2002a; Zhan *et al.*, 2002; Price, 2003; Skinner and Luckman, 2004; Desta, 2005; Giri *et al.*, 2005; Jonathan *et al.*, 2005; Stefanov and Netzband, 2005) however the specific applicability of these methods to the area and context characterizing this study is not known yet.

The present study can be seen in the framework of CORINE land cover database-update effort. Of interest is the possibility to use the developed methodology to aid CORINE's future updates; additionally the terms and conditions of the integration of medium resolution solutions have to be investigated. What needs to be assessed before monitoring based on medium resolution solutions can become operational is the degree of information loss compared to monitoring with high resolution data. Having assessed this loss, the question remains if the so with resulting land cover product can fully substitute the higher resolution alternative or if rather an integration of both products is recommended. What is more, it has to be understood what would be the gain in information thanks to the higher temporal frequency with which medium resolution data are made available and eventually if this gain is relevant for land cover monitoring on the European scale. For this specific study the question is if MODIS data are able to tell us everything that Landsat data can, or if instead critical information disappears which can only be won back with the help of the higher resolution images (Price, 2003).

Eventually, indications provided by this material should contribute to the development of a monitoring concept to identify future land cover changes within Europe as delineated in the BIOPRESS initiative. BIOPRESS is one of the thematic projects which are being carried out within the framework of the initial phase of the Global Monitoring for the Environment and Security (GMES) programme. The GMES initiative aims at achieving this 'European capacity for Global Monitoring for the Environment and Security' by 2008. BIOPRESS will produce information on historical (1950 - 1990 - 2000) land cover change in and around a large sample of Natura2000 sites and translate this information into pressures on biodiversity. The focus of the project is to develop a standardised product that will be extendable to Europe (<http://www.creaf.uab.es/biopress/index2.htm>).

In this material, special emphasis is given to the results obtainable for the urban land cover class ("Artificial Surfaces" in CORINE's Nomenclature). A number of reasons support this choice. First and foremost, urbanization falls within the six key pressures on biodiversity in European regions on which BIOPRESS will concentrate. The others being: abandonment, afforestation, deforestation, drainage, intensification (arable) (Hazeu and Mücher, 2005). Moreover, it has been demonstrated that urbanization is the phenomenon for which the link between land cover changes and the pressure on biodiversity is most straightforward (<http://www.creaf.uab.es/biopress/index2.htm>). Last but not least, it has to be reminded that CORINE land cover 2000 update identified the changes for this class as the most significant for Europe.

1.3. Research Objectives

General objective

The scope of this study is to assess the utility of medium spatial resolution satellite data (MODIS/Terra Surface Reflectance Daily 250m Product) in the spatial-temporal dimension for land cover mapping and identification of change signals in the northern part of Italy. This potential has to be seen in the context of CORINE land cover database-update effort.

Specific objectives and research questions

To fulfil the aforementioned general research objective this study should provide the answer to a number of specific questions. These questions helped defining the specific objectives of this study as presented in the following.

First, given the methodological framework of this study which sees MODIS data missing for the year 1990, the question has to be answered if these can be reproduced starting from Landsat TM 1990 images. It follows that one objective is to develop a methodology to simulate MODIS data for the year 1990 and assess the accuracy of this simulation.

Second, a sound approach for classification of the remote sensing datasets based on the Maximum Likelihood classification algorithm has to be developed. This will help answering the question of which accuracy can be reached by this classifier for the specific study area and for the different land cover classes. Specific attention will be paid to results for the urban land cover class.

Third, the authors are interested in answering the question if improvement of classification accuracies becomes noticeable when exploiting the multitemporal dataset. This will be done by comparing classification results of MODIS single-date versus multitemporal datasets.

Last but not least, our objective is to interpret and evaluate the results of the post-classification automated change detection. The question is if this change detection approach has been feasible for this study and how accurate its results are compared to the change figures provided by CORINE.

1.5. Research hypothesis

The MODIS 250m daily reflectance product has potential to function as an alarm product signalizing land cover-use conversion occurring at the European scale.

1.6. Report Structure

Chapter one describes first a general introduction to the topic followed by the specification of the research problem, research objectives and hypothesis. The findings of the literature review which helped broaden the understanding for the topic are presented in chapter two. Chapter three outlines the data and methodology adopted in this study of which an overview is given by the methodological conceptual model. The methodology is divided into pre-processing, simulation of MODIS data for the year 1990, classification of the remote sensing images for time one and time two and eventually post-classification change detection. Results of the simulation, classification and change detection are presented and discussed in chapter four. Chapter five summarizes the main conclusions as derived from this study and provides recommendations for further research in the field of land cover monitoring and change detection.

2. Literature Review

2.1. *Land Cover Monitoring and Remote Sensing*

2.1.1 Land Cover/Use Change

Land cover can be defined as the biophysical attributes of the earth's surface, which can roughly be separated into natural features, such as water, vegetation, desert, ice, etc. and artificial physical features, including mine exposures and settlements. Land use is the human purpose or intent applied to these attributes. Land-cover and land-use changes can be indicative of transformation from one cover or use type to another, in which case we speak of a conversion process or the preservation of the general cover or use type which however undergoes modifications in its structure, which we call a modification process. While long-term climatic changes due to astronomical phenomena and short-term variations resulting from phenological cycles can be considered naturally driven, other changes are introduced by human activity (Baulies and Szejwach, 1997; Lambin *et al.*, 2001).

At no other time in history land cover and land use alteration has been as fast and wide-ranging as in the last 50 years (Reid *et al.*, 2005). The magnitude and spatial reach of those changes is so significant that, when aggregated globally, they considerably influence key aspects of Earth System functioning. Biotic diversity worldwide, local and regional climate change as well as global temperature rise, soil degradation and the ability of biological systems to support human needs are all aspects influenced by changes in land use/cover (Lambin *et al.*, 2001).

While not denying the improvements in land cover characterizations made possible by better data derived by remotely sensing systems, many are still the challenges in land cover mapping and monitoring. The first challenge can be summarized in the attempt of integrating and synthesizing land cover information worldwide. Different definitions adopted around the world for specific land cover classes complicate this attempt. Focusing on the class forest for example it has been traced that more than 90 definitions exist throughout the world (Lepers *et al.*, 2005). A further problem hindering a complete and consistent overview of land cover is the varying spatial resolution with which changes are recorded around the world or in the same areas

over time. Long time monitoring studies will always have to deal with the change in technology and in methods which although usually meaning an improvement also represents a type of unwanted discontinuity. Eventually, varying temporal and spatial coverage of data sets causes an unbalanced focus of attention towards some parts of the world which appear to be more interested by rapid modifications simply because they have been monitored more intensively. Many parts of the world are still not adequately represented in the available datasets, fostering the possibility that rapid change is occurring in locations that are currently not identified (Lepers *et al.*, 2005).

As emphasized by Lambin (2001), an additional problem is the frequently missing understanding of the causes behind an identified change which are reported to be frequently simplified or mistaken leading to the wrong policies being formulated. Taking deforestation as one of the most common and popular land cover alterations it has often been explained as triggered by the ‘push’ of population growth and poverty to invade and cut the forest. Not denying a responsibility of the latter phenomena, deforestation particularly in tropical areas is more probably linked to changing economic opportunities caused by social, political and infrastructural changes (Lambin *et al.*, 2001).

The European continent falls within the regions most comprehensively and consistently monitored for what regards land cover. Statistics have shown that in the last 10 years 2.9% of the total surface (approximately 85500 ha) has changed in land cover (Weber & Hazeu, 2004). However, large differences exist among and within countries for what regards the extent of land cover change and the dominant change trajectories. Remaining on the continent scale, an important land cover conversion trend is urban sprawl mainly at the expense of agriculture land; the centre of this phenomenon lies on the Atlantic and Mediterranean coasts. General farmland abandonment is another occurring phenomenon, as is, to a lesser extent, the creation of new agricultural land. The Mediterranean coastal zones are one such exception, where urban pressures near the coast results in intensification of agriculture towards the inland marginal zones. Last but not least, changes in forest land seem to be balanced, with felling activities and conversions roughly equalling the same amount of surface characterized by formation of young forest (Weber & Hazeu, 2004).

2.1.2. Instrument Properties Influencing Land Cover Mapping

Satellite-based data have been determined to be a cost- and time-effective resource to document changes over large geographic regions. Nevertheless, still no optimal combination of data type and analytical method can be identified as being the most successful across broadly variable ecosystem conditions (Zhan *et al.*, 2002; Lunetta *et al.*, 2004; Rogan and Chen, 2004). Among the challenges when designing or choosing an instrument for land cover monitoring is the choice for the most suitable combination of spatial, radiometric/spectral and temporal characteristics. This combination will determine the size and the type of the recognizable land cover changes (Townshend and Justice, 1988). What limits this choice is the data volume which has to be kept at manageable proportions to make the data transfer from the satellite to the receiving station practicable. This means that the expert has to set preferences for what regards the dimensionality of the spatial, spectral and temporal data properties. What is more, the time and cost factor have also to be kept in mind (Rogan and Chen, 2004).

The question if a higher spatial resolution leads automatically to a better representation of the land transformation is answered affirmatively by some authors (Townshend and Justice, 1988), while others are more cautious underlining the effects of shadow fraction and of the increase of local variance (Woodcock and Strahler, 1987). Besides this, a higher spatial resolution usually means that the period separating two images depicting the same area will increase to match the repeating coverage of the sensor and can expand even more due to cloud cover problems. In change detection studies, the temporal frequency of coverage should optimally approximate the change-rate of the phenomenon or land cover class we want to monitor to avoid to incur in excessive omission errors. For example if focusing on vegetation for areas that undergo rapid regeneration, the spectral signatures of regenerated vegetation can be difficult to differentiate from previously existing vegetation, if analyzed over long time intervals (Lunetta *et al.*, 2004). Moreover, the radiometric sensitivity of the instrument controls the size of radiance differences that are detectable and thus also the discernable changes (Townshend and Justice, 1988). It is therefore easily understandable that it would not be wise to point only on the spatial

properties of the data so with loosing key advantages offered by the temporal and spectral dimensions.

It should be remembered that the concept of spatial resolution is strongly interlinked with the concept of measurement scale of the observation (Woodcock and Strahler, 1987; Herold *et al.*, 2002a) and thus for those applications where the operational scale, required to reach the study purpose, is easily determined so is also the desired spatial resolution of the remotely sensed datasets. For instance when interested in changes taking place at the urban scale, the highest spatial resolution is recommended, as this probably will be more determinant than the spectral or temporal properties of the data. On the other side, when working on the global scale, the expert will point on spectral and temporal analysis reducing the spatial resolution of the data. This is not the case for application at an intermediate scale level for which a less obvious answer is provided and the choice becomes more ambiguous (Price, 2003). For studies dealing with the effect of spatial resolution on the ability to monitor the status of land cover and land cover change we refer to the work of (Townshend and Justice, 1988; Pax-Lenney and Woodcock, 1997a; Price, 2003), however the reader should be warned that no overall guidelines will be provided but rather case-specific indication.

Following these considerations we conclude that the change product is a function of the actual transformations occurred on the earth surface and the properties of the remote sensing instrument used for monitoring and that the latter ones have to be chosen carefully.

2.1.3. Mapping of Urban Land Cover

As reported in the United Nations' World Urbanization Prospects (2004 revision), approximately half of the world population lives in urban areas and this is anticipated to exceed 60% by 2030 (United Nations' World Urbanization Prospects, 2004 In: Tatem *et al.*, 2005). Consequently, a wrong even if for long time alleged assumption in the context of land transformations is the one that sees urbanization as unimportant in global land cover change. Given its relatively small percentage compared to other

land cover/use types, urban areas occupy less than 2% of the earth's land surface, land change studies often fail to take it into account concentrating more on land cover classes such as agricultural or forested areas (Lambin *et al.*, 2001). What has been disregarded however is that changes in urban areas as such, trigger many other land cover modifications which somehow are interlinked with it, thus encompassing a much wider area as the one effectively occupied by urban land cover. Only the awareness of the existence of a so called 'rural-urban linkage' will allow urban areas to be reconsidered as central pawn in land change assessment studies (Lambin *et al.*, 2001).

Considering that the development of urban areas (expansion in area, increase in population, changes in economic and social structures) trigger large modifications of land surfaces and reach across geographic borders, an increase desire to monitor their dynamics is being observed in the scientific community (Herold *et al.*, 2002a). To succeed in this attempt a clear identification of what is considered an urban area has to be developed. Currently urban areas are identified in different ways based on land area, population density and spatial arrangement, but more and more the use of image-processing methods based on spectral response is becoming a valid means for their delineation. Earlier applications of remote sensing data for urban land cover mapping have mainly been restricted on one hand to fine resolution data focusing on the local scale and on the other hand on coarse resolution data for global scale applications. For what concerns the first category, extensive use has been made of the Landsat series of sensors (Multispectral Scanner - MSS, Thematic Mapper - TM and Enhanced Thematic Mapper Plus - ETM+) which however limits these studies to small areas (Schneider *et al.*, 2003; Stefanov and Netzband, 2005). For what concerns the second category of applications a number of important products can be mentioned. These include the Digital Chart of the World (DCW) urban layer which although valuable dates back to 1960; maps derived from the Defence Meteorological Satellite Program Operational Linescan System (DMSP-OLS); and eventually night time lights data which present the disadvantages of a coarse resolution (2.7 Km), poor registration and blooming effects corresponding to city boundaries (Schneider *et al.*, 2003).

Several authors (Ben-Dor *et al.*, 2001; Herold *et al.*, 2002a) have lamented the difficulty of mapping urban sites as these areas are characterized by small extents and fragmented shapes with an indistinct spectral pattern compared to other land cover categories. Few studies have focused on the issues of spectral properties of urban land cover types and their representation and mapping from remote sensing data and those that have, attributed to this class, highly complex and diverse spectral properties. Reason behind is the heterogeneity of the urban environment, typically consisting of built up structures (e.g. buildings, transportation nets), multiple diverse vegetation covers (e.g. parks, gardens, agricultural areas), bare soil zones and water bodies. Accordingly, an unambiguous "spectral urban signal" is not obtainable (Herold *et al.*, 2002a; Herold *et al.*, 2002b). Generally, it has been observed how spectral separability of urban land cover types is strongly dependent on spectral sensor characteristics (Herold *et al.*, 2002a; Herold *et al.*, 2002b; Ben-Dor *et al.*, 2001).

Speaking of the spatial properties, it is important to understand how monitoring of the urban class is a strongly scale-driven process which becomes especially challenging when coarsening the spatial resolution of the employed remote sensing instrument (Herold *et al.*, 2002a). Meentemayer in his work of 1989 defined scale as the spatial and temporal dimension of an object or process and termed it crucial to geographic analysis (Herold *et al.*, 2002b). Herold and Clarke distinguished four meanings of 'scale' depending on the context in which it is been used, these are: cartographic scale, geographic scale, operational scale and measurement scale. As geographic scale, if we focus on urban area mapping, we understand the spatial extent of the study area. The image pixel size or more simply the image spatial resolution expresses the so called measurement scale. The combination of the spatial heterogeneity of the target land cover structures and the sensor spatial resolution determine eventually the level of geometric detail in land cover representation by remotely sensed data and consequently the scale at which the created classification product can be employed, also known as operational scale. For more detailed indications on the scale factor in relation to monitoring different phenomena at different spatial resolution we refer to the work of Woodcock and Strahler (1987).

2.2. **Medium Resolution Satellites: MODIS**

From the early 1980s to the present monitoring of the terrestrial environment and especially of vegetation relied mostly on AVHRR of the NOAA series of platforms. Data from the Landsat series of sensors started in 1972, have been extensively used in land cover and land use studies (Townshend and Justice, 2002; Vermote *et al.*, 2002). Building on these experiences and urged by the need of filling the gap existing between high and coarse resolution sensors in 1999 the first MODIS instrument was launched on board of NASA's EOS Terra satellite, followed three years later by MODIS on the Aqua satellite (Justice *et al.*, 2002; Townshend and Justice, 2002). The MODIS/Terra instrument compared to its predecessors shows substantial enhancements in spatial resolution, number of spectral channels, choice of bandwidths, radiometric calibration and quality of derived products (Townshend and Justice, 2002). Moreover, its orbital configuration and viewing geometry deliver daily complete global coverage apart from the equatorial region where the repeat frequency is approximately 1.2 days (Justice *et al.*, 2002; Zhan *et al.*, 2002). The first seven of its 36 spectral bands are designed primarily for remote sensing of the land surface, of which only band one (red, 620-670 nm) and band two (near infrared, 841-876 nm) have a spatial resolution of 250 m (Justice *et al.*, 2002; Zhan *et al.*, 2002). Bands 3 through 7 are natively 500m resolution.

Several advanced land products are being generated using these bands. Particularly, the red and near infrared bands, given their higher spatial resolution and their position in the electromagnetic spectrum (Zhan *et al.*, 2002), are most interesting for change detection studies. These bands have been combined in a value-added product for monitoring of land conversions, known as the Vegetative Cover Conversion (VCC) product. A composite product derived from 250-meter resolution 16-day composites from the Terra/MODIS instrument constitutes the intermediate product for the VCC dataset. The intermediate 16-day composites are generated from daily, level 2G, surface reflectance data (MOD09), and are composited based on the quality of the daily observations as determined by the QA flags in that product. The MODIS VCC product is generated four times per years (quarterly) and is designed to be a global alarm product for land cover conversions. Where land cover conversion is defined as the cumulative effect of human and natural event over time, not including changes

related to seasonal or phenological changes in vegetation. Nonetheless, it should be noted that this product is not intended for areal quantification of land cover changes but rather functions as an alarm product able to reveal the need for further investigations by means of higher resolution data. A number of factors have been identified as possible source of errors in this product, among those the presence of clouds which were not flagged in the QA layer of the input data and inter-annual variability affecting vegetation are worth mentioning (User Guide for MOD44A VCC: <http://glcf.umiacs.umd.edu/data/modis/vcc/>). For an extensive assessment of the VCC product we refer to the work of Zhan *et al.* (2002) in which three land cover conversion cases, namely detection of burned areas, detection of flooding/flood retreat and detection of deforestation, were analyzed. The study revealed the suitability of MODIS's VCC product to detect the occurrence of change in a specific zone (Zhan *et al.*, 2002).

MODIS's VCC product has not been used for the present study, one reason being its unavailability for the time frame under investigation (1990–2000). An additional reason is that composite data may have larger misregistration errors than the data used in this material. As emphasized by Zhan (2002) the misregistration error of individual images is likely to propagate into the composite image and result in lower geometrical accuracies thereof. In view of these considerations, this study has been performed on MODIS's surface reflectance product, defined by Vermote *et al.* (2002) as the reflectance that would be measured at the land surface if there were no atmosphere. This product is based on the MODIS L1B as the primary input and performs corrections for the effects of gaseous absorption, molecules and aerosol scattering, coupling between atmospheric and surface bi-directional reflectance function (BRDF) and adjacency effect (atmospheric point spread function) (Vermote *et al.*, 2002). The MODIS products represent the first global terrestrial products that are available and have been systematically atmospherically corrected and bidirectionally corrected for a sustained period of time (Townshend and Justice, 2002). Artefacts caused by the atmosphere were already accounted for in products used by the oceanographic community whereas the terrestrial community has been slow to develop procedures. The reason behind this delay is probably due to the relative influence of the atmospheric signal which results to be much stronger over water bodies than it is over land (Townshend and Justice, 2002). Despite the fact that the majority of the bands

designed for the MODIS instrument were specifically meant to satisfy the needs of the land community, compromises were made in the design of some bands used by both the land and oceans research communities. Notwithstanding the trend towards smaller, single mission satellites, for the expected future operational imagers will remain multi-purpose thus calling for similar compromises (Justice *et al.*, 2002).

In general, the potential of MODIS data for land cover monitoring and change detection has been widely acknowledged in literature (Justice *et al.*, 2002; Townshend and Justice, 2002; Vermote *et al.*, 2002; Zhan *et al.*, 2002; Skinner and Luckman, 2004). Nevertheless, it has to be reminded that other moderate spatial resolution sensors (with resolutions between 250 m and 8 km) have become operational in recent years as well. Their limited success compared to MODIS could be attributed to the more complicated access to users because of charging policies, mission lifespan and acquisition strategies. These instruments include the Vegetation instrument on board the French SPOT mission, the POLDER instrument on board ADEOS 1, SeaWifs, the Advanced Along Track Scanning Radiometer and MERIS of the European Space Agency's ENVISAT. The majority of these sensors were intended principally for oceanographic applications with the inclusion of bands useful for remote sensing over land (Townshend and Justice, 2002). For what concerns the MERIS instrument of the European Space Agency ENVISAT platform, with its 15 bands it acquires images in the VIS and NIR part of the electromagnetic spectrum at a full resolution of 300 m or a reduced resolution of 1.2 Km (Clevers *et al.*, 2004). Although very meaningful for deriving land cover information, MERIS data products are for the time being intended primary for research activities and thus require temporal, spatial and quality verification pre-processing. On the other hand, MODIS surface reflectance data are highly processed products and in most of the cases do not require further pre-processing prior to image classification (Skinner and Luckman, 2004). Preliminary studies conducted by Mücher (Personal comment, 2005) have shown that similar land cover classification accuracies are obtained when using MERIS and MODIS data. These results are confirmed by a study conducted by Clevers (2004) in which a Principal Component Analysis was performed on MERIS images. The Principal Component result revealed that 99% of all information is already contained in the first two Principal Components, where the first had high positive loadings for the bands in the near-infrared region and the second for bands in the visible region. Those regions

of the Electromagnetic Spectrum (ES) roughly correspond to those available from the MODIS sensor at a comparable spatial resolution. Moreover, by studying the correlation coefficients between MERIS's spectral bands Clevers *et al.* observed that bands in the visible region of the ES are highly correlated the same as bands in the near-infrared part of the ES. This last observation further supports the fact that the higher amount of bands at full resolution of the MERIS instrument compared to those available at comparable resolution from the MODIS instrument are not value adding for the purpose of land cover monitoring.

Eventually, we can conclude that the potential of monitoring the terrestrial environment at moderate spatial resolution has been acknowledged but not fully exploited and thus numerous research opportunities are still present in this field.

2.3. *Change Detection Techniques*

Singh (1989) defined the process of change detection as the recognition of differences in the state of an object or phenomenon by observing it at different moments in time (Singh, 1989 In: (Lu *et al.*, 2004). Few years later Green (1994) recommended that the interpreter should not limit himself to observing but additionally try to control all variances caused by variables that are not of interest so as to be able to analyze only those changes resulting by differences in variables of interest (Green *et al.*, 1994, In: Lu *et al.*, 2004). Digital change detection is based on co-registered multi-temporal remote sensing images and relies on the premise that transformations in land cover or land use have as consequences variations in radiance values and that these variances prevail over radiance changes resulting from other factors such as differences in atmospheric conditions, differences in sun angle or differences in soil moisture (Mas, 1999).

Several authors have summarized and reviewed the existing change detection techniques (Mas, 1999; Lu *et al.*, 2004) of those the most known ones are grouped and briefly described in the following. The here with proposed categories are main simplifications and different authors differ in their choice.

Within the so called algebra category, algorithms require the user to specify a threshold value to determine the areas of change. Among these the most known is image differencing but other common techniques are image regression, image rationing, vegetation index differencing, change vector analysis (CVA) and background subtraction.

An additional category requiring a threshold-definition is the transformation category which includes Principal Component Analysis (PCA), Tasseled cap, Gramm–Schmidt (GS), and Chi-square transformations. The easy implementations of algebra methods and the reduction in data redundancy of transformation procedures have made these techniques common in change detection studies. In more recent years however, these techniques have been replaced by more complex ones, preferred because providing a complete matrix of change information (Lu *et al.*, 2004). To obtain a complete matrix of change information the classification category of techniques is the most suited. It includes post-classification comparison, spectral–temporal combined analysis, expectation–maximization algorithm (EM) change detection, unsupervised change detection, hybrid change detection, and ANN. These methods are based on classified images and thus depend on the accuracy of this process starting from the quality and quantity of training sample data (Lu *et al.*, 2004).

Many more change detection techniques exist, but their in depth review is outside the scope of this study. An important consideration is that none of the existing techniques can be considered as performing best for all applications. Many are the factors that influence change detection studies and this explains the fact that often different authors obtained different results when testing the same technique. Generally we can conclude that it is partly the aim of the study which determines which change detection technique is most appropriate. If the aim is a rapid qualitative change detection analysis, visual interpretation can result most suited. On the other hand if change/no-change information by means of digital change detection is what we want to achieve, single-band image differencing and PCA represent the best choice. Eventually for a detailed ‘from-to’ detection, post-classification comparison is the recommended method to adopt given that sufficient training sample data are available. Having defined the aim of the present study, the approach considered most suited is the post-classification change detection method. This method has been recommended

among others by Petit and Lambin (2001) as the most suited for change detection applications interesting a long time period for which data of different sensors have to be used. Multi-source data do not represent a problem as each data layer can be generalized to a common land cover scheme prior to comparison, minimizing in this way environmental, sensor and atmospheric differences.

In a comparative study by Mas (1999) post-classification comparison was evaluated against the most known methods for change detection using Landsat MSS images. The technique was found performing best over algebra techniques (image differencing and vegetation index differencing) and transformation techniques (Principal Component Analysis). The lower accuracy obtained with the latter procedures was attributed to their inability to differentiate the variations of soil moisture and vegetation phenology from variations due to land cover changes. This problem is not encountered when performing independent classifications where classes with different signatures at different times of the year can still be assigned to the same land cover class (Mas, 1999). Last but not least, as mentioned earlier the post-classification approach has the strength of providing a complete matrix of change information. In the present study the interest lies not only on where and in which extent changes have occurred but also on which are the classes losing and gaining in importance over time.

3. Materials and Methods

3.1. *Study Area and Time Interval*

The test area we have chosen for this study is located in the northern part of the Italian peninsula; delimited by the Alpine mountain chains in the North and by the Apennine mountains in the South this area is also known as the Po valley, basin of the river Po which from the Alps eventually ends up in the Atlantic sea. The basin encompasses the regions Piemonte, Val d'Aosta, Lombardia, Emilia Romagna, marginal areas of Liguria, Veneto and Trentino (see Figure 1). With a surface of 69979 km², of which 29372 km² in low land, this area was in the past mainly covered by forest intermittent only by swamp areas. Today we can find cultivated land interrupted by extensive concrete patches located in correspondence of the urban centres. The choice of this area as suitable for our study is not casual but driven by the delicate condition of this territory, territory which is considered the area that in Italy preserves the less signs of what once was the original landscape. Human activity has transformed this area in such a way that its balance can only be granted by a high contribution of energy and resources coming from outside the system. Natural calamities have often interested this land sending alarm signs of the incorrect use of the territory. Starting from the 1980ies more attention has been paid to the development of this area with the formulation of policies at the national and European level aimed at its conservation (directive 92/43/CEE). These and future policies which will contribute to the responsible management of the Po' valley are for the biggest part based on remote sensing land cover and land use monitoring activities similar to the present one (<http://www.legambiente.com>).

In view of the fact, that the prime interest of this study is the understanding of the changes affecting the Po valley in the 1990-2000 time interval, the developments of the urban class have been selected as being the most significant indicators thereof. As extensively described in section 2.1. the effect of the modifications interesting this class are being reflected on a much wider area as the one effectively occupied by urban land cover. Focusing especially on the class urban is therefore believed to provide a trust worth indication of the developments in the area and at the same time respecting the resources and timeframe available for the completion of this study.

The reason behind the choice of the ten year period spanning from 1990 to 2000 is twofold. Firstly, considering a shorter time interval would not provide us with sufficient change indications due to the slow transformations-rate of European land cover. Secondly, we are interested to compare the here obtained land cover product with CORINE change DB, whose first version dates 1990 and whose update followed 10 years later.



Figure 1 Location of the study area, north Italy

3.2. Data

3.2.1. Remote Sensing data

MODIS

In order to perform this work, daily Terra/MODIS atmospherically corrected surface reflectance data were acquired, containing red and near-infrared bands and corresponding metadata at 250m resolution (product ‘MODIS/TERRA SURFACE REFLECTANCE DAILY L2G GLOBAL 250M SIN GRID V004’ or abbreviated MOD09GQK). The properties of this product are summarized in Table 1 whereas

general MODIS specification can be consulted in Appendix 1. In order to select the best quality data (cloud free and free of instrument recording errors) images were first browsed by means of the ‘MODIS Land Global Browse Image’ web source (<http://landqa2.nascom.nasa.gov/cgi-bin/browse/browse.cgi>). Eventually, three images acquired respectively on April 22, June 20 and September 10 of the year 2000 could be downloaded from the NASA Earth Observing System (EOS) Data Gateway (<http://edcimswww.cr.usgs.gov/pub/imswelcome/>). Subsequent to downloading the image quality could once more be assessed by reading the metadata contained in the quality flag band.

The resolution of the two MODIS bands corresponding to the visible red and the near infrared (NIR) is 250x250m and their centre in the electromagnetic spectrum is 645 nm and 858 nm respectively. We are also provided with three bands of additional information on band quality, orbit and coverage, and number of observations (<http://www.yale.edu/ceo>). Reflectance products typically provide an estimated “at surface” spectral reflectance, equivalent to a ground-level measurement with no atmospheric scattering or absorption. The correction algorithm accounts for atmospheric gases, aerosols, and thin cirrus clouds. Version four (V004) products are validated, meaning that product uncertainties are well defined over a range of representative conditions and thus are ready for use in scientific research.

Table 1 Terra/MODIS surface reflectance product characteristics

| | |
|-------------------|-----------------------|
| Product type | MOD09GQK |
| Product level | 2G |
| Collection | V004 |
| Data type | 16 bit signed integer |
| Actual data range | -100 to +16000 |
| Fill value | -28,672 |
| Units | reflectance |
| Grid | 4800x4800 row/column |
| Projection type | Sinusoidal |
| Image area | Tile h18v04 |
| File format | HDF-EOS |

Landsat

Landsat products utilized in this study are TM and ETM Top Of Atmosphere (TOA) data, which were downloaded free of charge from the Global Land Cover Facility (GLCF) at the University of Maryland (<http://glcfapp.umiacs.umd.edu/index.shtml>). Five scenes are required to cover the whole study area; these are acquired in the summer months of the year 1990 (+/- two years) for what concerns the TM scenes and 2000 for ETM scene (see Table 2). Images taken in late spring or summer (from June till September) are preferred because cloud cover is believed to be less and because most arable land is already covered by vegetation allowing distinguishing it from urban areas.

Table 2 Landsat TM and ETM+ scene specific acquisition dates

| Scene | Calendar date (dd/mm/yyyy) | |
|---------|----------------------------|------------|
| | TM | ETM+ |
| 192_029 | 07/08/1991 | 20/06/2000 |
| 193_028 | 16/08/1992 | |
| 193_029 | 12/09/1990 | |
| 194_028 | 31/08/1989 | |
| 194_029 | 04/07/1991 | |

The selected images for this study are GeoCover products. GeoCover data is Landsat data which has been orthorectified and processed to a higher quality standard. The process of orthorectification removes erroneous image displacements caused by the interaction between terrain relief or local elevation changes and sensor orientation variations. Datasets are Level 1 Geometrically Corrected (L1G) products, this means they are free from distortions related to the sensor (e.g., jitter, view angle effect), satellite (e.g., altitude deviations from nominal), and Earth (e.g., rotation, curvature). For the effects derived from the presence of the atmosphere however no correction has been made (TOA data). GeoCover data currently represent the most accurate commercially available base maps with worldwide coverage (Tucker *et al.*, 2004).

For this study work was carried out with only two of the seven Landsat bands, precisely band 3 (red band) and four (near infrared band), available at 30 m spatial

resolution. Each Landsat band is saved as a single file in the GeoTIFF format and data is provided in rescaled 8-bit unsigned integer (DN) values.

3.2.2. Land cover datasets

CORINE

CORINE land cover vector datasets interesting the Italian peninsula have been obtained accessing the European Environment Agency (EEA) home page (<http://dataservice.eea.eu.int/dataservice/>). The following three geo-referenced databases are acquired for the present study:

- CLC 1990 DB,
- CLC 2000 DB and
- CLC 1990-2000 change DB,

respectively representing the first version of the database, its update and the change database. These datasets differ for what regards the materials and methods behind their creation. The original methodology was based on the image-interpretation on 1:100,000 image printouts in which a transparent film was overlapped over the images and digitized at the end of the image interpretation process (Perdigao and Annoni, 1997). A method, relying on the hardcopy inventory from image printouts with no or only limited use of image processing and GIS software, proved to be the most feasible approach at the time corresponding to the start of the program (mid eighties). Nonetheless, such an approach, requiring two intermediate hardcopy products (satellite images and transparencies) prior to obtaining digital results, made the occurrence of errors likely especially during the digitalization process. By the time of the update of CORINE Land Cover Data Base (CLC DB) in the year 2000, technical developments had made it possible to introduce computer technologies throughout the process of building the inventory (softcopy). The display of the data on computer screens contributed to make the process more efficient in view of time and cost factors and increased the achievable accuracy (Bossard *et al.*, 2000). It is understandable then that the two CORINE products hold different geometrical accuracies, with the updated version representing the enhanced product.

In both phases, the aid of ancillary data has been crucial to the interpretation, these have comprised any documentary, cartographic or photographic information

concerning land cover which does not come directly from the satellite database (Perdigao and Annoni, 1997). Some general figures about the program are summarized in Table 3.

Table 3 The CORINE land cover project in figures (source: CORINE land cover Technical Guide, Bossard *et al.*, 2000)

| | |
|----------------------------|---|
| Area covered | 2.3 millions km 2 12 countries from 62° N (The Faeroes) to 28° S (Canary Islands) from 14° W (Canary Islands) to 29° E (Kastellorizon) |
| Working scale | 1/100000 1 500 standard map sheets using 10 different projection systems |
| Area smallest mapping unit | 25 hectares more than 700000 basic unit (polygons) vector data-base around of 1 gigabyte |
| Land cover nomenclature | three levels first level: five headings second level: 15 headings third level: 44 headings |

3.3. Methodological Conceptual Model

The methodology developed for this study follows the scheme depicted in Figure 2 where input data are Landsat's and MODIS satellite images and CORINE land cover thematic maps. Five main steps can be distinguished in the work flow, namely pre-processing, simulation of the missing dataset, classification, validation of the classification and change detection.

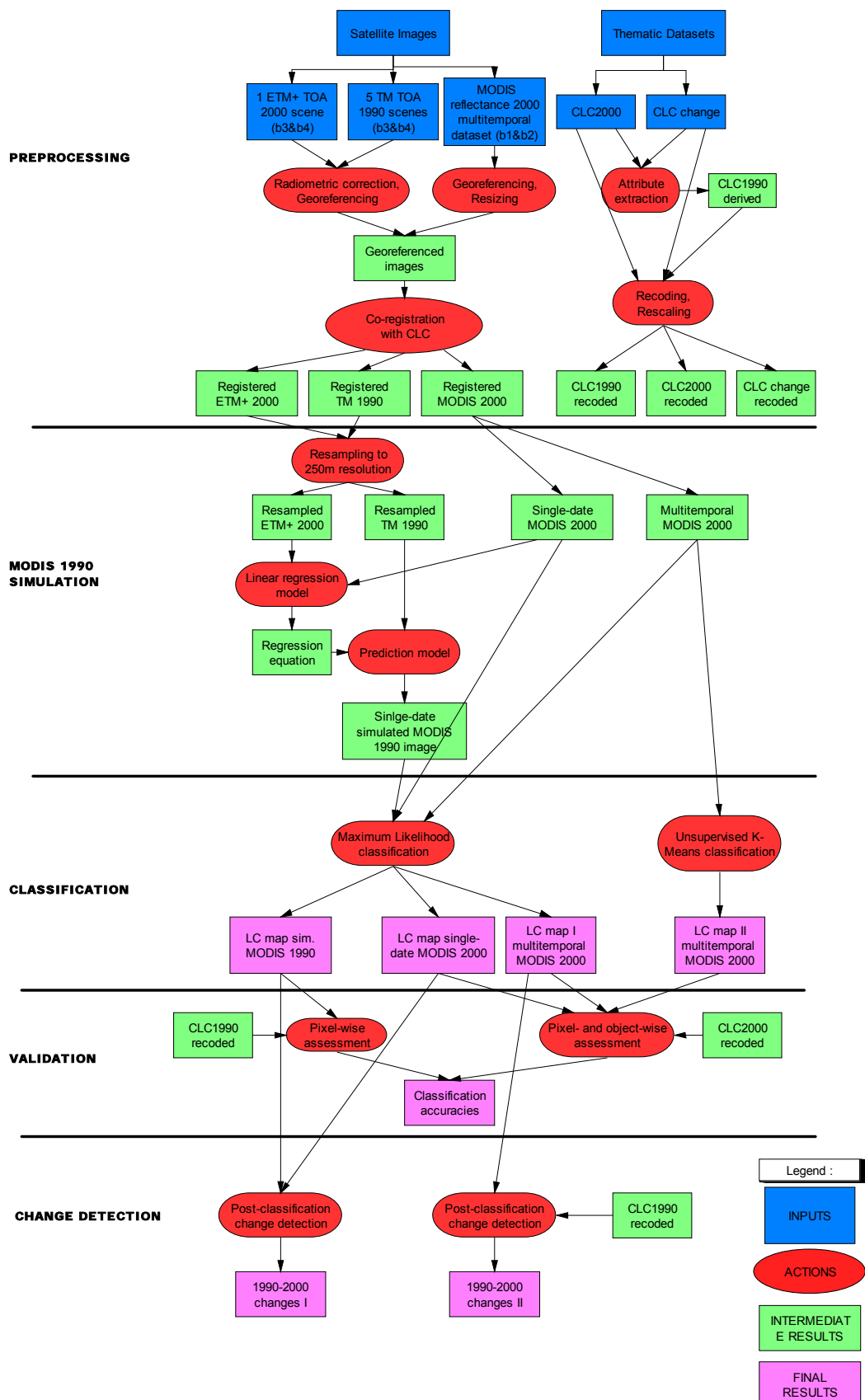


Figure 2 Flow chart of working scheme

3.4. Preprocessing

For the pre-processing of the remote sensing datasets the commercial software package IDL-ENVI version 4.2 has been used, whereas the preparation of the land cover vector datasets has been accomplished in ArcGIS version 9. With the pre-processing the aim was to make data spatially and spectrally comparable as required by the final change detection stage.

3.4.1. MODIS

As a first step of the data preparation the three MODIS images have been reprojected to *Albers Conical Equal Area WGS1997* coordinate system. Reprojection is necessary because the MODIS Level 3 product is generated as grided output in the Sinusoidal projection which is unique to MODIS land products and is not accommodated by most of the conventional “off the shelf” software used for image processing and spatial data analysis. The MODIS Reprojection Tool (MRT) version 3.2a running on Linux platform has been used for this purpose. During this step, the original MODIS data format, namely HDF-EOS format, was converted to the standard ENVI image format. Eventually, datasets were transformed to a valid reflectance data range by dividing the cell values by 10,000. These data were then stored with a float data type of 4 byte real (Justice *et al.*, 2002).

Although, the original downloaded scenes encompass mountainous areas (Alps and Apennines), for the actual classification and change detection process our interest lies mostly in the flat plane (Pianura Padana) as it is there that most urban centres are situated. In view of this, the study area will be successively restricted to areas with low relief and thus topographic normalization was considered not necessary for this study.

3.4.2. Landsat

For what concerns Landsat data the pre-processing has been some what more time consuming because it involved also the radiometric aspect of the data. The two main steps have been the radiometric calibration and the reprojecting to different coordinate

system. As aforementioned Landsat data are GeoCover products and this means that images have been orthorectified prior to distribution (<http://glcfapp.umiacs.umd.edu/index.shtml>).

Radiometric calibration

For what concerns Landsat's initial product status it has to be mentioned that when processing L0 products to L1 products, the pixel values from the raw unprocessed image data are converted to absolute radiance using 32-bit floating-point calculations. Before output to the distribution media the absolute radiance values are eventually rescaled to 8-bit values representing calibrated digital numbers.

In the present study, digital numbers have been converted in physical units of apparent reflectance whose values can be compared from image to image. This is required because the area of study is larger than a single scene (precisely 5 scenes) and because different scenes taken over a period of years are being compared for change monitoring (Edwards, 1999). For this study only the first two steps of radiometric correction, namely the conversion from DN values to spectral radiance and from the latter one to apparent reflectance, have been carried out. The third step, known as atmospheric correction, has been omitted because not retained necessary for this specific application; justifications supporting this belief have been found after reviewing the work of different authors and are summarized in the following. As underlined by Song *et al.* (2001), whether an atmospheric correction is mandatory or not is determined by the information desired and by the analytical methods used for its extraction. A typical example of a remote sensing application for which the removal of the atmospheric effect is not needed is image classification when a maximum likelihood classifier is employed interesting a single date image. Assuming that the training data and the image to be classified are on the same relative scale (corrected or uncorrected) the influence of a correction will not be striking for classification accuracies. Likewise, when applying postclassification change detection, as is the case for this study, atmospheric correction is not necessary due to the fact that we are comparing maps which have been obtained by independent classifications (Song *et al.*, 2001). That is why for this study, classifications have been performed independently for each individual scene with the mosaicking interesting solely the thematic outputs.

Besides the fact that the removal of the atmospheric effect is not essential for the present work, it is also considered not very feasible in the given framework. No overpass-concurrent atmospheric data (e.g. aerosol content, atmospheric visibility) was available that could be used as inputs into radiative transfer models (RTM), such as 6S (Edwards, 1999). Also, with only two broad spectral bands available in the VIS/NIR, the empirical estimation of the necessary atmospheric optical properties for an RTM correction was not possible (Clark and Pellikka, 2004). Ideally, a method that uses in situ or ground-truth information is the most accurate in terms of correcting for atmospheric haze effects (Chavez, 1988). In the present study, we are working with remotely sensed data that have already been collected and therefore only methods that require exclusively information contained in the digital image data were considered. Among those, the most commonly employed is the Dark-Object Subtraction method. In this technique the minimum DN value in the histogram from the entire scene is attributed to the effect of the atmosphere and is subtracted from all the pixels (Chavez, 1988; Song *et al.*, 2001). However, if the dark objects, which usually are represented by water bodies, are not uniformly distributed across the scene, the assumption at the base of this technique of a constant haze value throughout the entire image can not be made. For the present study, not all our Landsat scenes encompass water bodies which could function as dark objects, and for the ones that do, dark objects are mostly confined to one extremity of the image thus not representing the overall atmospheric conditions present over the area (see images in Appendix 3).

Based on these considerations, for this study atmospheric correction of Landsat scenes was retained more harmful than beneficial and thus was left out from the process.

The calibration of Landsat scenes has been performed by means of Interactive Data Language (IDL) scripting. This method was preferred over ENVI's automatic calibration due to the possibility to view the algorithms and input parameters behind the process (see IDL script in Appendix 5). All algorithms as reported in the following have been obtained by consulting the Landsat 7 Science Data Users Handbook

(http://ltpwww.gsfc.nasa.gov/IAS/handbook/handbook_htmls/chapter11/chapter11.html).

The conversion of the Landsat's TM and ETM datasets from DN values to at-sensor spectral radiance implies the knowledge of the original rescaling factors which are band specific satellite parameters that can be obtained from the image header or metadata file. Equation (1) was employed to obtain spectral radiance at the sensor's aperture. A more extended version of this equation is represented by equation (2).

$$L_\lambda = GAIN * QCAL + OFFSET \quad (1)$$

$$L_\lambda = L_{\min}(\lambda) + \frac{L_{\max}(\lambda) - L_{\min}(\lambda)}{QCAL_{\max}} QCAL \quad (2)$$

The second step in Landsat's radiometric calibration is the conversion from radiance to planetary (also known as at-sensor, apparent or exoatmospheric) reflectance. This allows us to remove the effect of time differences among image acquisition (this is done by including in the algorithm the cosine of the solar zenith angle) and moreover it accounts for differences in exoatmospheric solar irradiance. Equation (3) has been used to compute the combined surface and atmospheric reflectance of the earth (see Appendix 2 for details).

$$\rho_p = \frac{\pi * L_\lambda * d^2}{ESUN_\lambda * \cos\theta_s} \quad (3)$$

Reprojecting to different coordinate system

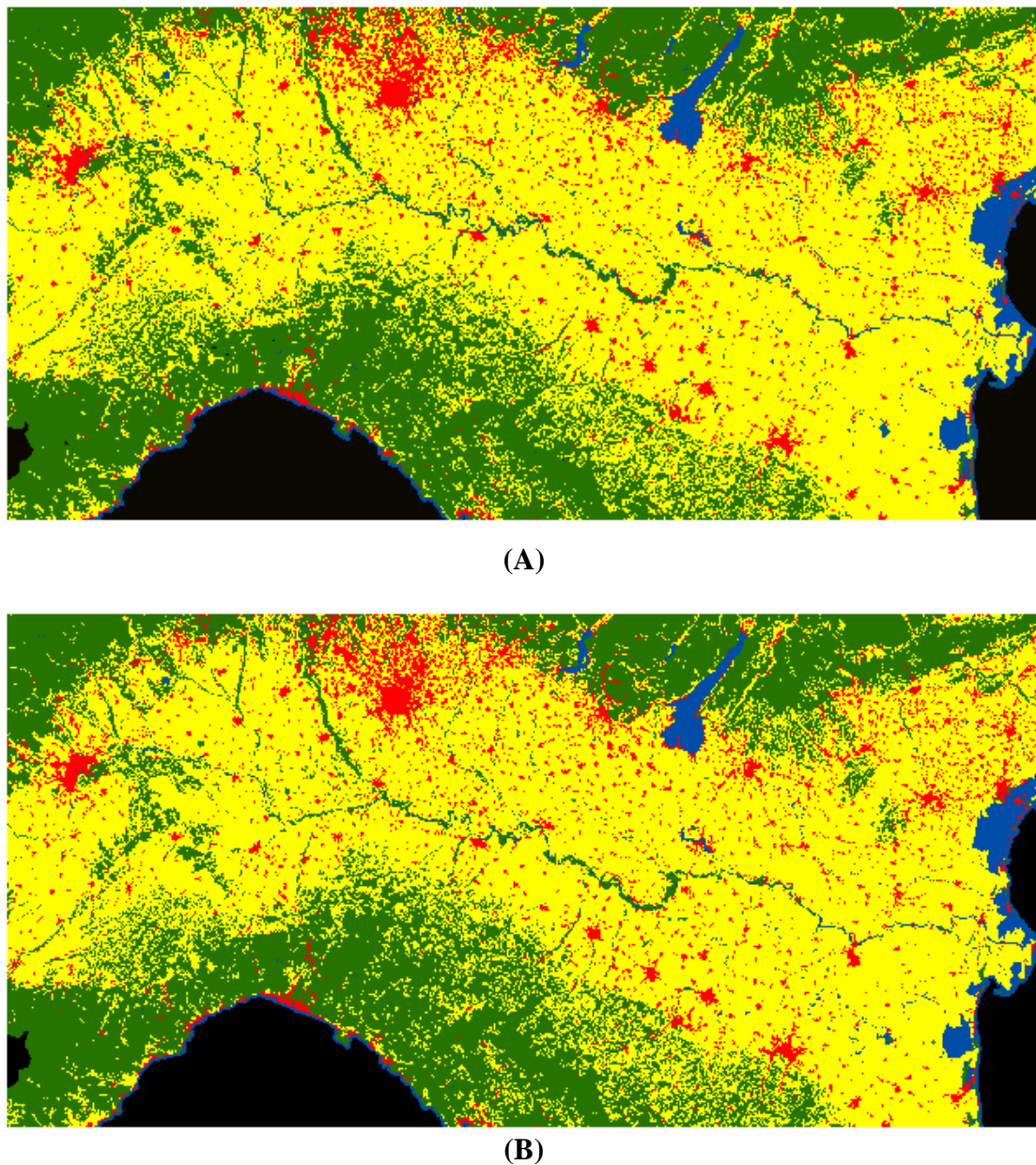
The Landsat TM and ETM images used in the present study are GeoCover products and thus georeferenced products. A simple transformation function will allow re-projecting the images from the current UTM (Universal Transverse Mercator) map projection (WGS84 datum) to the desired projection. The Albers Conical Equal Area projection (WGS72 datum) has been chosen for the present study. Eventually the red and near infrared bands will be combined for each individual scene into a multispectral image.

3.4.3. CORINE

The pre-processing of the thematic datasets has been performed in ArcGIS version 9. The first step consisted in verifying that CLC1990 and CLC2000 vector datasets were geometrically matching which unfortunately lead to the conclusion that the two datasets are systematically shifted from one another. This can be explained if we consider that CLC datasets are first saved in the country-specific projection and successively converted to a common European projection system; this process can easily have introduced inconsistency between our datasets. Moreover, as reported in section 3.2.2., the two products are generally characterized by slightly different geometrical accuracy. To overcome this problem CLC 1990 dataset was derived based on the remaining two available datasets: the CLC 2000 and the CLC 1990-2000 change datasets. The latter one includes only those polygons that have been updated and precisely it reports the land cover label attributed before and after the transformation. By performing a union operation, a datasets containing the information contained in both attribute tables was obtained. Successively, a new attribute (field) containing for each polygon the land cover class it belonged to during CLC 1990 creation was added. The next step is to recode the legends of CORINE datasets to a more general land cover classification scheme so as to define a set of meaningful classes effectively discernible with MODIS reflectance information. This procedure was performed with the aid of indications obtained from the unsupervised classification of the MODIS 2000 multitemporal dataset (see section 3.6.1.). The results obtained confirmed that working with only two bands restricts the number of classes that can be meaningfully distinguished. In view of this we decided to merge classes to match level 1 of CLC 44 class nomenclature (an overview of the complete class nomenclature can be consulted in Appendix 6). Additionally, class 4 and 5 of CLC level 1 nomenclature were merged because their distinction is not considered relevant for this study. Eventually, the four classes defined for MODIS classification are:

1. Artificial surfaces,
2. Agricultural areas,
3. Forest and semi natural areas, and
4. Water bodies and Wetlands.

Eventually, the vector land-cover polygons for both dates were rasterized to a 250 m grid, to match the resolution of the MODIS data (see Figure 3).



Legend CORINE land cover level 1

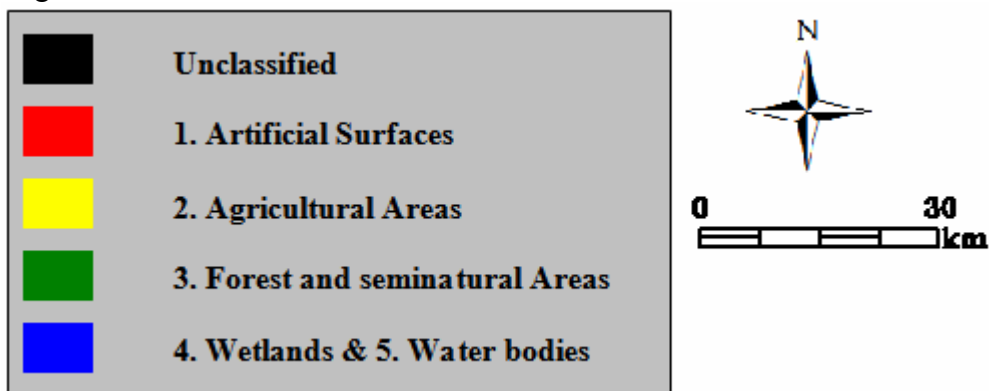


Figure 3 CORINE land cover classification images after recoding to 4 thematic classes (level 1 CLC Nomenclature). (A) 1990, and (B) 2000.

3.4.4. Datasets Co-registration

An accurate geometrical co-registration of images is the most critical image preprocessing requirement for monitoring land cover changes. The success of change detection studies is highly dependant on the precision of relative alignment between images that compose a multi-temporal data set (Stow, 1999). The variations among images that the registration process is aiming to get rid of are those due to the differences in image acquisition, not including those due to atmospheric conditions which can not be modelled by registration and in fact affect mostly intensity values and only for a minor part spatial characteristics (Stow, 1999). Image registration in brief consists in finding an adequate transformation so that the points in one image can be related to their corresponding points in the other.

For this study we decided to adopt an automatic image registration procedure as those offered by IDL-ENVI software package. This procedure uses so called Ground Control Points (GCPs). Ground control points are a set of selected pixels (or regions) that can be located accurately on both the image and the map; these are usually easily recognizable features such as intersection of roads, rivers or coastlines. Eventually the control points can be used to identify the transforms between the input image and the reference image or map (Chalermwat, 1999). The present study made it desirable to adopt the Image-to-Map registration option instead of the Image-to-Image one. When registering an image to a map coordinate system, the pixels can be referred in terms of map coordinates (latitudes and longitudes or easting and northing) this is often referred to as geocoding. The map coordinates were entered by means of CORINE land cover vector datasets. Reasons behind the choice of this approach were of different nature. Firstly, the problem in choosing the higher resolution satellite image as a reference, and thus adopting Image-to-Image registration, is that the warped image is automatically resembled to the base image spatial resolution which is not desired for this study. Secondly, given the framework of this study which is CORINE's update it is advisable to take the latter as reference for all our datasets. Landsat TM 1990 images were registered against CLC 1990 dataset, whereas CLC 2000 was used for Landsat ETM+ and MODIS image registration. It has to be reminded at this point that no difference in geometrical accuracy exists between the in this study employed CORINE dataset. This is due to the fact that, as reported in

section 3.4.3., CLC1990 dataset has been derived from the CLC2000 and the change database.

Ground Control Points (GCPs) identifiable on both the CLC reference datasets and the remote sensing scenes were precisely located with the help of a cursor. From the reference datasets the categories artificial surfaces and wetlands&water were found most suitable for point identification. A total ranging from 8 to 11 GCPs were identified for each individual Landsat scene, whereas a total of 18 points were selected for the MODIS image. Eventually the residual registration error (RMS) was computed and the points adjusted in order to maintain the acceptable error (Table 4).

Table 4 Registration settings for Landsat TM, MODIS and ETM scenes

| Base dataset | Warp images | Warping method | Resampling method | Scenes ID | GCPs | RMSE |
|----------------------|-----------------|--------------------------------------|-------------------|-----------|------|-------|
| CLC1990 (derived) | Landsat TM | Polynomial 1 st degree | Nearest neighbour | 192_29 | 8 | 1.491 |
| | | | | 193_28 | 10 | 1.695 |
| | | | | 193_29 | 11 | 1.607 |
| | | | | 194_28 | 8 | 1.588 |
| | | | | 194_29 | 9 | 1.503 |
| CLC2000 | MODIS | Polynomial 1 st degree | Nearest neighbour | | 18 | 1.382 |
| CLC2000 | Landsat ETM+ | Polynomial 1 st degree | Nearest neighbour | 192_29 | 10 | 1.396 |
| | | | | 193_28 | 9 | 1.618 |
| | | | | 193_29 | 9 | 0.863 |
| | | | | 194_28 | 9 | 1.695 |
| | | | | 194_29 | 8 | 1.813 |

One drawback in using control points in automatic registration is that it is not the easiest task to identify effective GCPs especially when working on relatively coarse images as is the case in this study. It has been demonstrated that the registration error decreases as the number of GCPs is increased (Chalermwat, 1999), on the other hand we also observed that the capacity to find satisfactory GCPs and with it the quality of GCPs accuracy decreases as their number increases.

In literature no undisputed opinion regarding the size of the tolerable registration error is found. Chalermwat (1999) defined an error of ± 1 pixel as acceptable in the co-registration of images for change detection application. For the present study, although acceptable accuracies are reached, a certain degree of bias resulting from the registration process is expected to influence the final change detection product. It should be reminded that an error of only one pixel in a Landsat image corresponds to a misplacement of about 80 meters distance on Earth (Tian 1986, In: (Chalermwat, 1999)).

To validate the accuracy of the registration CLC vector dataset were overlaid on the satellite images and a visual consistency check was carried out. In general it could be noticed that the datasets matched; some inaccuracies were detected in correspondence of line features, such as rivers, but those could be related to the fact that for the line elements the minimum width as specified by CORINE is 100 meters. Where this width was not reached, approximation might have been taken place during CORINE digitalization.

3.5. *Simulation MODIS 1990*

One of the challenges of the present study, which aims at performing change detection from 1990 to 2000 based on MODIS data, is the lack of time one data. Although MODIS's spectral channels interval were originally selected because they closely match the spectral band widths of Landsat's data facilitating intercomparison (Price, 2003), a direct 1:1 relation can not be established. For what concerns the visible red part of the EM spectrum, the MODIS sensor acquires the signal of slightly shorter wavelengths (0.62-0.67 μm) compared to the Landsat instruments (0.63-0.69 μm). The near infrared part of the spectrum covered by the Landsat sensors (0.76-0.90 μm) is much wider and encompasses the part covered by the MODIS instrument (0.84-0.88 μm). What is more the data generated by the two instruments differ in their spatial resolution, with Landsat recording at 30m and MODIS at 250m for band 1 and 2. Following these consideration it becomes clear how Landsat TM for the year 1990 can not be taken as substitute date one images for our change detection without any transformation taking place.

As in the majority of pioneer studies which precede their concrete applicability, some kind of simulation has to be carried out to be able to replace the yet missing component. In this study the missing component is represented by the MODIS data for the year 1990 and simulation has been performed by means of an empirical approach. Several mathematical approaches for data simulation are known to exist in literature but their complexity has been found not suitable for the timeframe in which this study has to be carried out.

Simple averaging of the fine resolution data to match the spatial resolution of the coarse resolution data will not produce data sets with comparable spatial information (Pax-Lenney and Woodcock, 1997a). This objective instead was achieved for this study by empirically modelling the association existing between Landsat and MODIS data for the year 2000 and successively exploiting the so with obtained prediction equation to derive MODIS 1990 from Landsat TM 1990 datasets. For deriving the empirical relation, the ETM scene whose acquisition date corresponds exactly to MODIS acquisition (20th June 2000) was used.

Resampling of the Landsat images from 30x30m to 10x10m pixel size using nearest neighbour was performed allowing preserving as much as possible the original reflectance of the image. Successively, Landsat 10m resolution data were upscaled to 250m by means of pixel aggregate which averages all of the pixel values that contribute to the output pixel. This method has been found most suitable when aiming at simulating different scale levels and has been confirmed in literature (Alexandridis and Chemin, 2002). Special attention was given to the origin of the resampling which was chosen to match exactly the origin of the corresponding MODIS pixel. This was achieved by resizing the Landsat image by means of map coordinates at 10m spatial resolution prior to the upscaling to 250m so as to attain maximum precision in the subsetting.

As a second step, MODIS 2000 and Landsat ETM 2000 data have been graphically screened to determine how their relationship can best be described; from the band specific scatter plots the data appeared to be related linearly (see Appendix 7). An ordinary linear regression analysis by means of SPSS statistical software was carried

out to explore the relationship; the independent or explanatory variable was represented by the ETM 2000 and the dependent variable by MODIS 2000 dataset. The goodness of the fit was assessed by means of the Pearson's correlation coefficient (R) which indicates both strength and direction of the linear relationship. The least square method was used in the attempt of finding the function that best approximates the data (a "best fit") by minimizing the difference of the original MODIS data versus the predicted ones, known as residuals. Assuming the model we fit to the data is correct, the residuals approximate the random errors. Therefore, if the residuals appear to behave randomly, it suggests that the model fits the data well. Whereas, if the residuals display a systematic pattern, it is a clear sign that the model fits the data poorly. For this method to be applicable we assumed errors in each measurement to be randomly distributed.

The model including an intercept has been compared with the no-intercept model by means of Pearson's coefficient (R), eventually linear regression through the origin was found to be the best fit for our data. The band-specific regression (least squares) equation of the line which best fits our data is of the type $y = \alpha x + \varepsilon$, where α is the unstandardized coefficient or slope and ε is the unpredictable component or error. Including observations of the explanatory variable (ETM) in the equation yields estimated values of the dependent variable (MODIS). To validate the reliability of our prediction the difference between the original MODIS and the predicted one, also known as residuals, was investigated.

The fact that the predicted values do not exactly match the original ones could have many explanations some of which are nor traceable neither explainable. One possible source that instead can indeed be verified is misregistration between our datasets. The fact that images have similar mean values strengthen the conviction that different spatial distribution of features has influenced the association between the images. Two independent approaches to verify this assumption were developed. In the first, images were upscaled to 500m spatial resolution by aggregation through averaging (Alexandridis & Chemin, 2002), in the second only big homogeneous features were considered to derive the correlation. Both approaches resulted in an improvement of the correlation strength between images and thus confirmed the influence of misregistration in lowering the association. This can easily be understood considering

that the particular study area is characterized by fragmented land cover, meaning that a mismatch of the order of one 250x250m pixel can already signify another land cover type.

For our model to be valid certain assumptions were made. First and foremost, we assumed that the subset area for which the transfer functions have been derived is representative of the whole study area. This assumption was made after visual investigation of the land cover distribution for the whole study area. Moreover, what can be considered the overriding assumption for the here developed simulation strategy, is the possibility to interchange Landsat TM and ETM data from a spectral point of view. This would mean that even though the regression model has been calibrated with ETM data its validity is further granted when using TM data. For further detail on ETM-TM comparison we advise to refer to '*Landsat-7 ETM+ as an observatory for land cover initial radiometric and geometric comparison with Landsat-5 Thematic Mapper*' by Masek *et al.* (2001).

3.6. Classification

In this section an overview of the methodology adopted for classification of our remotely sensed datasets is outlined. In general, two broad approaches can be distinguished in literature, namely spectral and contextual image classification. While the first category is based on the spectral response pattern associated with each individual pixel, the second one has as main study unit homogeneous regions also known as segments or objects.

An extensive review of the most significant scientific literature since the completion of this research revealed how object-oriented approaches have won in popularity in recent years but have merely interested high resolution data, most commonly data from the Landsat and SPOT family of sensors or in many cases also very high resolution solutions data such as IKONOS or Quickbird (Walter and Fritsch, 2000; Walter, 2004; Blaschke, 2005; Blaschke *et al.*, 2005; Moeller and Blaschke, 2005). In view of what just mentioned and of indications obtained from preliminary results, a pixel-based approach has been chosen for the present study.

Among the pixel based approaches, the Maximum Likelihood classification algorithm was found to be the most successfully applied in several studies (Cho, 2000; Kral, 2003; Jonathan *et al.*, 2005). In a study by Dwivedi *et al.* (2004) the most common classifiers of remote sensing data for land-use/land-cover mapping are evaluated, the MLC was found superior to all other methods except for artificial neural network techniques.

3.6.1. Unsupervised Classification MODIS 2000

The author decided to purposefully start the series of classification procedures with the unsupervised approach. This approach clusters pixels in a data set based on statistics only, without any user-defined training classes (RSI-ENVI, 2006). In this way a first impression of the land cover classes which can be discerned by an automatic classifier based on our dataset is obtained. These indications turned useful when working with the supervised approach in which a feasible number of classes, for which to collect training samples, have to be defined in advance. As mentioned in section 3.4.3., the results obtained with the unsupervised approach were as well employed for CLC class recoding.

This step has been carried out in ENVI using K-means unsupervised classification, a method which calculates initial class means evenly distributed in the data space then iteratively clusters the pixels into the nearest class using a minimum distance technique. Each iteration recalculates class means and reclassifies pixels with respect to the new means (RSI-ENVI, 2006). The parameters specified were the number of classes, set to four, the change threshold which was kept at the default value of five and eventually the maximum number of iterations, set to three. A mask encompassing clouds, snow and data-errors was applied to the multitemporal MODIS 2000 image prior to classification.

3.6.2. Supervised Classification MODIS 2000: Single Date versus Multitemporal Approach

The potential of the MODIS instrument for land cover monitoring on the European scale lies in its red and NIR bands which are characterized by 250m resolution. The low spectral dimensionality of our data restricted to four the number of classes considered in this study. To test whether a higher temporal resolution could eventually compensate for the small number of bands used, three MODIS scenes for different seasons where combined in a multitemporal dataset. The images were respectively from mid April, June and September of the year 2000.

The training stage

The same classification strategy was used to classify the multitemporal dataset and the single date image represented by the June acquisition. The number of considered classes was set to four corresponding to CORINE's higher nomenclature level with the exception of the class Wetlands and the class Water bodies which for the present study were merged in a single class as their distinction was not considered relevant. CORINE land cover vector datasets have been used as ancillary information in the classification process; it should here be remembered that we are mainly interested in developing an updating approach for CLC maps therefore the aid of the previous thematic datasets is most wanted. By overlaying CLC2000 vector dataset, recoded to the four-class nomenclature, over the MODIS image, training samples were defined. High importance has been given to the selection of representative training samples as this step has been indicated by some researcher (Dwivedi *et al.*, 2004) as more relevant than the type of algorithm eventually applied for classification. For the digitizing of the training fields individual polygons for specific classes were used. Hereby only the core areas of certain land-cover classes (without transition pixels) were used for creating spectral signatures, moreover areas within big and homogeneous polygons were preferred over small ones. This allowed lowering the effect of registration inaccuracies that exists between datasets. The number of samples has been taken proportionally to the class percentage as determined by CLC classification, with a higher number for the forest and agricultural class and a lower number for the less represented classes water and artificial surfaces.

Some indications of the spectral separability of our land-use/land-cover categories are provided by means of the calculation of the transformed divergence (TD) for our training samples. As reported in the ENVI User Guide (RSI-ENVI, 2006) TD values range from 0 to 2.0 and indicate how well the selected class pairs are statistically separated. Values greater than 1.9 indicate that the class pairs have good separability. For class pairs with lower separability values, it is recommended to attempt to improve the separability. A close look at the TD values in Table 5 reveals that the in this material used band combination, i.e. red and near infrared, does not represent the ideal set for achieving the desired classification accuracy when using a single-date image. Especially, for class pairs ‘Agriculture-Forest’ and ‘Urban-Agriculture’, for the single date dataset, a significant amount of spectral mixing is apparent. Although TD values generally improve when working with the multitemporal dataset, the only class pair for which a good separability is apparent (TD value= 2.000) is the ‘Agriculture-Water’ pair. It has also to be reminded that training samples generally represent the pure class spectral footprint and thus TD values based on the whole image are expected to be lower than the one reported in Table 5.

Table 5 Class Training Sample separability (Transformed Divergence)

| CLASS PAIRS | SEPARABILITY | |
|------------------------|--------------|----------------|
| | SINGLE DATE | MULTI-TEMPORAL |
| Agriculture vs. Forest | 1.214 | 1.921 |
| Urban vs. Agriculture | 1.748 | 1.975 |
| Urban vs. Water | 1.998 | 1.999 |
| Urban vs. Forest | 1.999 | 1.999 |
| Forest vs. Water | 1.999 | 1.999 |
| Agriculture vs. Water | 1.999 | 2.000 |

The classification stage

In view of the fact that the spectra of the defined land cover classes are close to one another in the measurement space and have high variance, a probability classifier is

preferred over a distance classifier. The Gaussian Maximum Likelihood classification algorithm (ML) has been chosen for this study as it quantitatively evaluates both the variance and covariance of the category spectral response patterns when classifying an unknown pixel (Lillesand *et al.*, 2004). What is more, following a literature review of comparable materials it turned out to be the favoured choice by several authors (Cho, 2000; Kral, 2003; Jonathan *et al.*, 2005). The basic ML algorithm is a purely statistical approach based on Bayes' theorem which assumes that the variables are continuous and follow a Gaussian or normal distribution (Jonathan *et al.*, 2005).

3.6.3. Supervised Classification simulated MODIS 1990

Following simulation of the '1990 MODIS dataset' we end up with 5 individual pseudo-MODIS scenes that need to be classified independently. Independent sets of training samples have to be collected for each scene considering that we are dealing with data not corrected for the atmospheric effect. Images were acquired in slightly different dates (it should be remembered that those were originally Landsat TM scenes) and therefore atmospheric conditions might not be exactly comparable.

As done for the MODIS 2000 dataset, four classes are distinguished and a maximum likelihood classification algorithm is applied. The so with obtained five thematic maps are eventually mosaicked into a unique dataset covering the full extent of the study area and their accuracy is evaluated against CLC 1990 dataset.

3.7. Accuracy Assessment

The following section provides the methodology adopted for the validation of the classification results. For the classification obtained from the MODIS 2000 multitemporal dataset, two validation approaches are compared: a pixel- and an object-based approach. The latter one aims at resembling more closely the methodological framework of the reference dataset, represented by CORINE's land cover map.

The accuracy of spatial data has been termed by the United States Geological Survey (USGS) as: “*The closeness of results of observations, computations, or estimates to the true values or the values accepted as being true*”. This definition implies already that what is called ‘true’ is sometimes dependent on the expert decision and therefore assumes a subjective dimension (Banko, 1998). Given the extent of the study area and the time at disposal for this research, field data, representing the most valid source of validation, could not be collected. Instead CORINE’s land cover maps obtained from high resolution Landsat data are used as ‘ground truth’ reference. It follows that, we are confident in making the necessary assumption that these data can be considered accurate for the purposes of this project.

3.7.1. Pixel based validation

A pixel-wise accuracy assessment has been carried out for the time 1 and time 2 classification results. For the 1990 classification, CLC1990 map has been taken as reference dataset, whereas for the 2000 classifications the CLC2000 thematic information is used as ‘ground truth’ to evaluate the performance of the algorithm. Confusion matrices, known also as contingency or error matrices, and from it derived indices were used as base for validation. The confusion matrix has been identified in literature as the core of classification accuracy assessment (Congalton, 1991; Foody, 2001; Lillesand *et al.*, 2004). As a simple cross-tabulation of the mapped class label against that observed in the ground or reference data, the confusion matrix provides not only class specific accuracies estimates but as well characterizes errors (Foody, 2001).

In the following a brief overview is given of the from the confusion matrix reported indices used in this study. The most commonly reported accuracy measures as found in literature is the percentage of cases correctly allocated known as ‘overall accuracy’. This is computed by dividing the total correct (i.e. the sum of the major diagonal) by the total number of pixels in the error matrix (Congalton, 1991; Foody, 2001). A major problem of this measure is that some cases may have been allocated purely by chance. To accommodate for the effect of chance agreement, a KAPPA analysis is

done whose result is known as KHAT statistics (K) and is obtained as depicted in equation (5). Developed by Cohen (1960) the Kappa coefficient verifies whether the results presented in the error matrix are significantly better than a random result. Kappa increases to one, as chance agreement decreases and becomes negative, as less than chance agreement occurs. A Kappa of zero occurs, when the agreement between classified data and verification data equals chance agreement. Contrarily to the overall accuracy measure which incorporates only diagonal elements of the error matrix, the kappa coefficient has the advantage to indirectly integrate the off-diagonal elements as a product of the row and column marginals (Congalton, 1991; Foody, 2001).

$$\hat{K} = \frac{N \sum_{i=1}^r X_{ii} - \sum_{i=1}^r X_{i+} * X_{+i}}{N^2 - \sum_{i=1}^r X_{i+} * X_{+i}} \quad (5)$$

where:

- r: number of rows and columns in error matrix,
- N: total number of observations,
- X_{ii} : observation in row i and column i,
- X_{i+} : marginal total of row i, and
- X_{+i} : marginal total of column i.

An additional weakness of the overall accuracy as only expression of the fidelity of a classification towards its reference target is its non-site-specific nature. As pointed out by Congalton (1991) in his extensive review of classification accuracy assessment, if all errors would happen to balance out themselves, a non-site-specific accuracy assessment will yield very positive but misleading results. Often very big accuracy differences exist within and among classes which can only be assessed by means of class specific indices. Intra- and interclass accuracies can be expressed from two standpoints giving rise to two measures known as producer's and user's accuracy. User's accuracy and producer's accuracy are the flip side of commission and omission errors, respectively. User accuracy is a percentage measure indicating the probability that a pixel included in a class actually represents that category on the ground. This measure is generated by dividing the number of correctly identified points (diagonal value) by the total number of points classified in that row. The more errors of

commission exist, the lower the user's accuracy as outlined in equation (6) (Banko, 1998).

$$\text{Users accuracy (\%)} = 100\% - \text{error of commission (\%)} \quad (6)$$

On the other hand, the producer's accuracy is a percentage measure of the omission error (see equation 7) it follows that the more errors of omission exist, the lower the producer's accuracy (Banko, 1998).

$$\text{Producers accuracy (\%)} = 100\% - \text{error of omission (\%)} \quad (7)$$

It indicates how accurate the class is compared to the reference data or how well the area was classified. This statistic is calculated by dividing the number of correctly identified points (diagonal value) by the total number of reference points in that column (Langley *et al.*, 2001).

3.7.2. Object based validation

For the MODIS 2000 multitemporal dataset an attempt has been made to simulate an object-oriented classification result starting from our pixel-based classification output. The thought behind this endeavour is that the employed validation strategy does not reflect the real disagreement between the two maps as long as one remains pixel- and the other object-based. To link the pixel-based land cover information obtained from the MODIS classification to CORINE's polygons a zonal statistics operation was performed in ArcGIS software. This operation allows assigning each of CORINE's polygons to the land cover class to which most of the classified MODIS pixels, falling within the polygon, belong to, by means of a majority rule. Eventually, MODIS polygon-wise classification has been validated by means of an accuracy matrix using as 'ground truth' dataset the CLC2000 map (see section 3.7.1. for details).

3.8. **Change Detection**

One objective of this study has been to compare spatial representations of two points in time, namely the years 1990 and 2000. This has been achieved by controlling as much as possible variance resulting from factors of no-interest (instrument differences, geometrical mismatch, etc.) and at the same time measuring the variance caused by land cover modifications in the study area. To do so an algorithm which simply compares two classification maps based on class pairs specified by the analyst has been employed. For each Initial State class, the algorithm identifies the classes into which those pixels changed in the Final State image. Changes are summarized in a change detection report consisting of three statistics tables (see Table 12 and Table 13 in section 4.3.), expressed as ‘Pixel Count’, ‘Percentage’ and ‘Area (square Km)’ respectively, listing the Initial State classes in the columns and the Final State classes in the rows. For each Initial State class (i.e., each column), the table indicates how these pixels were classified in the Final State image (RSI-ENVI, 2006).

A number of figures can be extracted from the change report of which the most significant are explained in the following. The Class Total row indicates the total number of pixels in each Final State Class, and the Class Total column indicates the total number of pixels in each Initial State Class. The Class Changes row indicates the total number of Initial State pixels that changed classes and is obtained by subtracting the number of pixel for a particular class which did not change from the Initial to the Final State from the Class Total column for that particular class. The Image Difference row is the difference in the total number of equivalently classed pixels in the two images, computed by subtracting the Initial State Class Totals from the Final State Class Totals. An Image Difference that is positive indicates that the class size increased (RSI-ENVI, 2006).

In addition, a special type of mask image (classification masks) that provides a spatial context for the tabular report is produced. The class masks are ENVI Classification images with class colours matching the Final State image, making it easy to identify not only where changes occurred but also the class into which the pixels changed (RSI-ENVI, 2006).

The choice of performing a map-to-map instead of an image-to-image comparison was made based on the ‘from-to’ information that can be obtained by the first and not by the latter technique (Lu *et al.*, 2004). Nevertheless, map-to-map comparison, also known as post-classification change detection, holds the disadvantage to be strongly influenced by the assumptions behind the individual classifications. Differences caused by discordant classification strategies and accuracies will be added to the actual land cover differences and introduce bias in the change recognition (Cho, 2000). Additionally, misregistration, as anticipated in section 3.4.4., can certainly be claimed as an ‘all times present’ source of error for change detection studies (Brown, 1992; Stow, 1999; Chalermwat, 1999).

For the present study change detection has been performed twice to differentiate between the single-date and the multitemporal datasets. The main reason behind this division lies in the time-dictated impossibility to simulate a multitemporal dataset for the year 1990. Moreover, the authors were interested in investigating the aid of the multitemporal approach to land cover mapping and monitoring. In view of what just mentioned, the first change detection was performed between the classification image based on the simulated single date MODIS 1990 data (time 1) and the classification obtained from the original MODIS 2000 single date data (time 2). On the other hand, in a second step change detection was performed between the CLC1990 dataset (time 1) and the classification image derived from the multitemporal MODIS 2000 data (time 2). For the latter case, we are well aware that maps which have been obtained on base of images taken by different instrument with different recording features are being compared. The so with obtained two change datasets were eventually compared among each other and with CLC change dataset for validation.

4. Results and Discussion

4.1. *Simulation MODIS 1990*

In this section the relationship between ETM 2000 and MODIS 2000 reflectance data is discussed on the basis of the results of the least squares regression analysis. Table 6 shows the models and coefficients. The comparison of the best fit of the models is determined based on Pearson's correlation coefficient (R).

Table 6 Regression models for MODIS 1990 simulation

| Model | Band | Regression equation | R | R Square | RMSE |
|----------------|-------------|---------------------------------|----------|-----------------|-------------|
| b \neq 0 (1) | red | y=0.972x+0.001+ ε * | 0.632 | 0.399 | 0.032 |
| | NIR | y=1.339x+0.027+ ε | 0.886 | 0.784 | 0.055 |
| b=0 (2) | red | y=0.98x+ ε | 0.941 | 0.885 | 0.032 |
| | NIR | y=1.441x+ ε | 0.988 | 0.976 | 0.055 |

* ε : unpredictable component (error)
 (1) Intercept model
 (2) No-intercept model

As anticipated in section 3.5., least square regression through the origin has been chosen as giving the best correlation results for this study. This choice was made based on the indication provided by Pearson's correlation coefficient for which the regression models with out intercept revealed higher correlation for both bands. Particularly for the red band, high improvement of the Pearson correlation was obtained (from 0.632 with intercept model to 0.941 with no-intercept model, Table 6). This choice can moreover be justified by assuming that both Landsat and MODIS data present zero reflectance value for very dark objects, such as water bodies; this assumption was also verified in the datasets in empirical way. In general, we can conclude that a Pearson's coefficient of 0.941 for the red and of 0.988 for the NIR band indicates the presence of a high correlation (> 0.9) between Landsat ETM+ and MODIS data acquired on the same date and encompassing the same study area.

For what concerns the R square values, of 0.885 and 0.976 for the red and the NIR band respectively, we can conclude that a high proportion of the variability in the

dependent variable about the origin can be explained by the regression. It has although to be pointed out that those values can not be compared to R Square for models which include an intercept. The graphical representation of the Root Mean Square error of residuals shows a nearly random distribution of residuals. However, what is of concern is the order of magnitude of the standard error of the regression, 0.032 and 0.055 for the red and NIR band respectively (Herold *et al.*, 2002a).

Several factors are known which could be liable for biasing the correlation between images acquired by different sensors. Particularly, for what concerns Landsat ETM+ and MODIS data some of those factors can be excluded whereas others have to be acknowledged. For instance differences in sun angle and view angle which are due to differences in time overpass can not be at the origin of de-correlation. The time lap between the Landsat ETM+ and the MODIS overpass is only of approximately 15-25 minutes (Alexandridis and Chemin, 2002) for images acquired the same day, too short for a change in climatic conditions been able to influence the land cover signal. On the other hand, the different processing that images could have been undergoing prior distribution certainly has lead to differences affecting the correlation. Last but not least, mis-registration represent a factor which certainly has influenced negatively the correlation, especially if considering that images have not been registered against each other but to a third dataset (CORINE 2000) and this could have generated an even larger mismatch (in case the errors are opposite in direction).

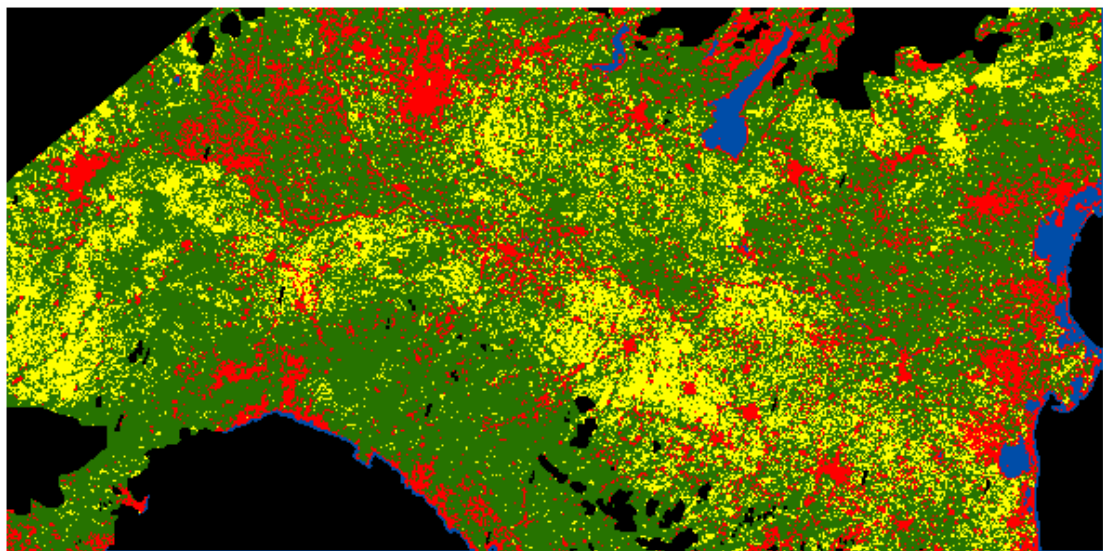
Eventually, these findings and considerations provide us with an indication of the degree of accuracy we are working with when performing MODIS's 1990 simulation using the so derived transfer equations. It should be recognized that further discrepancies might exists between the products of those two instruments. Regrettably, those are considered of unpredictable nature and can not be accounted for in this study, consequently will represent the uncertainty of our model.

4.2. Classification

4.2.1. Unsupervised classification MODIS 2000

From a first visual analysis of the classification image resulting from the K-Means classification algorithm, it becomes clear how all four CORINE Level one Nomenclature classes have been recognized by the automated classifier. Nevertheless, even when employing the multitemporal dataset, some confusion among classes is apparent as revealed by Figure 4. Particularly, the classes '*Agricultural Areas*' and '*Forest and semi-natural Areas*' show a significant overlap based on the dataset used for classification. Confusion between these two classes is quite common in land cover mapping studies and in this case is shown by an exaggerated prevalence of the forest over the agricultural land cover. The occurrence of forested area especially in the Po` valley, mainly characterized by agricultural fields interrupted by urban conglomerates, is an indication for the need of a training stage to improve the performance of the classifier. Results for the urban class show an overrepresentation; for this class as well as for the previous ones, a training stage is expected to be determinant in reducing the bias of the findings. Last but not least, the water class is mainly affected by the loss of the Po` river which is wrongly classified as urban. For this confusion the authors are not confident that a supervised approach will improve the result significantly, this is due to the conviction that it is the insufficient spatial resolution more than the spectral properties to mislead the outcome.

The conclusions drawn from the visual analysis are confirmed by the confusion matrix presented in Table 7. The overall accuracy of the classification is quite low, with only around 50% of the total pixels being classified correctly and a kappa value of 0.355. Class specific accuracies reflect the abovementioned observations.



Classification Legend

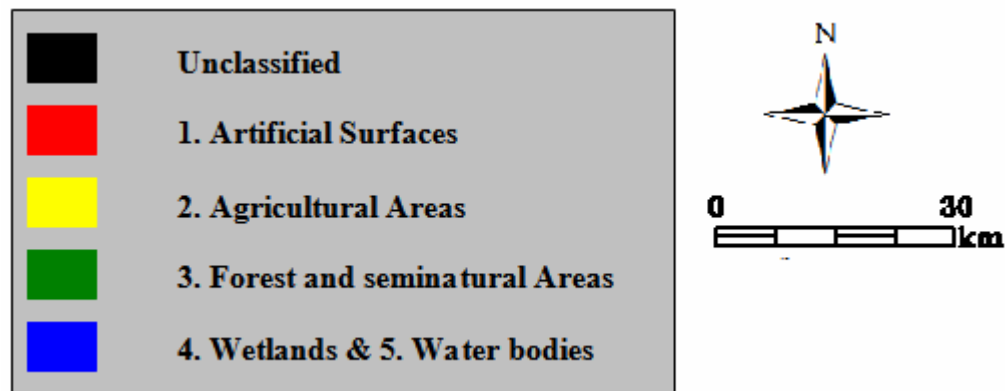


Figure 4 Classification image MODIS 2000 multitemporal dataset using K-Means unsupervised approach

Table 7 Confusion matrix MODIS 2000 multitemporal dataset using K-Means unsupervised approach versus CLC2000 ‘ground truth’

| Overall Accuracy= (627947/1247395)= 50.3407% | | | | | | |
|---|------------------------------|--------------------|---------------------|----------------|---------------|--------------|
| Kappa Coefficient= 0.3557 | | | | | | |
| Class | Ground Truth (Pixels) | | | | | |
| | UNCLASSIFIED | 1ARTIFICIAL | 2AGRICULTURE | 3FOREST | 4WATER | Total |
| Unclassified | 192720 | 0 | 0 | 0 | 0 | 192720 |
| 1Artificial | 5 | 41726 | 73316 | 34556 | 7254 | 156857 |
| 2Agriculture | 1 | 5697 | 174569 | 16932 | 322 | 197521 |
| 3Forest | 12 | 32523 | 444903 | 197943 | 1916 | 677297 |
| 4Water | 616 | 408 | 551 | 436 | 20989 | 23000 |
| Total | 193354 | 80354 | 693339 | 249867 | 30481 | 1247395 |

| Ground Truth (Percent) | | | | | | |
|-------------------------------|---------------------|--------------------|---------------------|----------------|---------------|--------------|
| Class | UNCLASSIFIED | 1ARTIFICIAL | 2AGRICULTURE | 3FOREST | 4WATER | Total |
| | (Percent) | | | | | |
| Unclassified | 99.67 | 0 | 0 | 0 | 0 | 15.45 |
| 1Artificial | 0 | 51.93 | 10.57 | 13.83 | 23.8 | 12.57 |
| 2Agriculture | 0 | 7.09 | 25.18 | 6.78 | 1.06 | 15.83 |
| 3Forest | 0.01 | 40.47 | 64.17 | 79.22 | 6.29 | 54.3 |
| 4Water | 0.32 | 0.51 | 0.08 | 0.17 | 68.86 | 1.84 |
| Total | 100 | 100 | 100 | 100 | 100 | 100 |

| Class | Commission | Omission | Commission | Omission | | |
|---------------------|-------------------|------------------|-------------------|-----------------|--|--|
| | (Percent) | (Percent) | (Pixels) | (Pixels) | | |
| Unclassified | 0 | 0.33 | 0/192720 | 634/193354 | | |
| 1Artificial | 73.4 | 48.07 | 115131/156857 | 38628/80354 | | |
| 2Agriculture | 11.62 | 74.82 | 22952/197521 | 518770/693339 | | |
| 3Forest | 70.77 | 20.78 | 479354/677297 | 51924/249867 | | |
| 4Water | 8.74 | 31.14 | 2011/23000 | 9492/30481 | | |

| Class | Prod. Acc. | User Acc. | Prod. Acc. | User Acc. | | |
|---------------------|------------|-----------|---------------|---------------|--|--|
| | (Percent) | (Percent) | (Pixels) | (Pixels) | | |
| Unclassified | 99.67 | 100 | 192720/193354 | 192720/192720 | | |
| 1Artificial | 51.93 | 26.6 | 41726/80354 | 41726/156857 | | |
| 2Agriculture | 25.18 | 88.38 | 174569/693339 | 174569/197521 | | |
| 3Forest | 79.22 | 29.23 | 197943/249867 | 197943/677297 | | |
| 4Water | 68.86 | 91.26 | 20989/30481 | 20989/23000 | | |

4.2.2. Supervised Classification MODIS 2000

In this chapter the results of the maximum likelihood classification for the MODIS single-date image and the multitemporal dataset for the year 2000 are presented. Classification images can be viewed in Figure 5 and Figure 6 respectively. Given the fact that the same training sample set was used for the two approaches, results are directly comparable by means of confusions matrices (see Table 8 and Table 9) with no need for normalization (Congalton, 1991) and thus are here discussed concurrently. Additionally, for the MODIS multitemporal dataset the pixel-level classification result has been resampled to CORINE's object-level. In view of this, in the following two sections are distinguished: the first reporting the validation for the original pixel-wise classification, while the second for the polygon-wise aggregated result.

4.2.2.1. Validation of pixel-wise results

A close look at the confusion matrices (Table 8 and Table 9) reveals an overall agreement between the obtained classifications and the CLC2000 thematic dataset, with an about 10% positive difference of the multitemporal approach over the single-date case. The in literature (Foody, 2001) commonly recommended 85% target was nearly reached by the classification of the multitemporal dataset which resulted in 84.44% overall accuracy versus the 74.11% obtained with the single-date dataset. When off-diagonal elements of the confusion matrix are included in the calculation of the kappa coefficient, accuracy reaches 0.593 and 0.741 for the single-date and multitemporal approach respectively.

Concentrating now on inter-class accuracies, the confusion matrices reveal how classes which are less represented on the terrain, namely urban areas and water (including wetlands), are the one that are mostly affected by error. Especially, it can be seen that for these classes the omission error is significantly higher than the commission error. For the urban class the omission error equals 70.68% (for the single-date image) and 74.60% (for the multitemporal approach), whereas the commission error reaches 52.44% (for the single-date image) and 34.21% (for the

multitemporal approach). The same information is inherent in the low producer's accuracy characterizing these classes, which even worsen for the multitemporal approach, sinking to 25.40% for the urban class and 59.05% for the water class. These results lie in accordance with the findings of Turner *et al.* (1989) in which it appeared that rare classes disappear as resolution becomes coarser (Pax-Lenney and Woodcock, 1997a). In agreement with what observed by Pax-Lenney and Woodcock (1997a) we observed how for our study area, large classes grow larger with increasing cell sizes (agriculture) whereas small classes diminish (urban, water). Additionally, it can be assumed that the rate of loss is influenced by the spatial patterns of the landscape at the fine resolution, with dispersed classes (urban, water) disappearing more rapidly than clumped classes (forest, agriculture).

The latter findings support the conviction that the spatial factor is within the factors at the origin of the discrepancy observed between MODIS 2000 classification images and CLC2000 datasets. It follows that the disagreement found following a straightforward comparison of these two dataset, is to be linked to the different scales at which these two land cover products should be interpreted more than to errors. The scale factor, is particularly affecting less represented classes such as urban and water classes, whose small and scattered objects are been suppressed in mixed-pixel as the cell resolution increases. An example is provided by the unilateral confusion which results in more than half of the urban pixels being wrongly classified as agriculture pixel (65.45% for the single-date image and 71.45% for the multitemporal dataset). The visual analysis confirms that the small urban centres scattered across the wide agricultural plane of the Po valley are lost to the agricultural class whose objects are of far larger dimension. The same can be observed for the water and wetlands category which experiences a substantial loss due to the insufficient size of its elements, as an example the Po river is not detected by the classifier. These observations are in accordance with the conclusions drawn by Gallego (2001) when comparing CLC database with a land cover product obtained from higher resolution images. Gallego emphasized the fact that pixel-wise disagreement can be very misleading as both maps can be perfectly consistent with each other, and have a high % of disagreement by pixel because they represent the same reality at different scale. It follows that area estimation of land cover classes by simply adding the area of the polygons labelled as belonging to that class does not have any meaning if not related

with the scale of the land cover map it refers to. A drop of the urban class from 6.4% to 2.5% (area decreases from 502212.5 ha to 195056.25 ha) and of the water class from 2.4% down to 1.5% is observed when comparing class occurrence as obtained from CORINE and as obtained from the MODIS classification. The dominant land cover classes, namely forest and agriculture, on the other hand experience either almost no change in occurrence or a slight increase (agriculture).

The second main aspect believed to be at the origin of the discordance between our classification and the reference data is the spectral factor. As earlier revealed by the training sample separability figures in section 3.6.2., a certain overlap between the agriculture and forest class and between the agriculture and the urban class is present. The confusion between these class pairs is believed to be in part due to the low spectral dimensionality of the finest spatial resolution MODIS product. In an attempt to lower inter-class confusion, the high temporal resolution of the MODIS product is exploited when working with the multitemporal dataset. However, it has to be underlined how at times contradictory findings have been reported by authors concerning the aid of temporal profiles for class identification. Temporal data series have been found improving the identification of especially agricultural classes characterized by seasonal response by some authors (Pax-Lenney and Woodcock, 1997b) whereas no aid to their identification has been recognized by others (Langley *et al.*, 2001). For the present study, the separability between agricultural and forest areas improved as a result of multitemporal data series and most important the omission error of the class agriculture decreased from 26.92% to 9.1%. In general it can be observed that the commission error decreases for all classes causing an overall rise of the user's accuracy, whereas the producer's accuracy improved only for classes whose response is affected by seasonality. As revealed by Jonathan *et al.* (2005) non-seasonal classes such as urban and water categories benefit less from a multitemporal approach. Moreover, it has to be reminded that for this study images corresponding to only three dates (April, June and September) have been combined while other studies (Pax-Lenney and Woodcock, 1997b; Jonathan *et al.*, 2005) have investigated the potential of extended time series. Extended time series allow certainly identifying a greater amount of class specific features as has been the case for this study. Having acknowledged this, it is not surprisingly how some classes are still confused with the multitemporal dataset. Particularly for the urban class it can be hypothesized that

urban areas characterized by lack of vegetation cover and thus low reflectance in the NIR part of the EM Spectrum have been at times confused with agricultural fields left ‘resting’ (i.e. unused in order to recover) and thus resembling the spectrum of bare soil (Jonathan *et al.*, 2005).

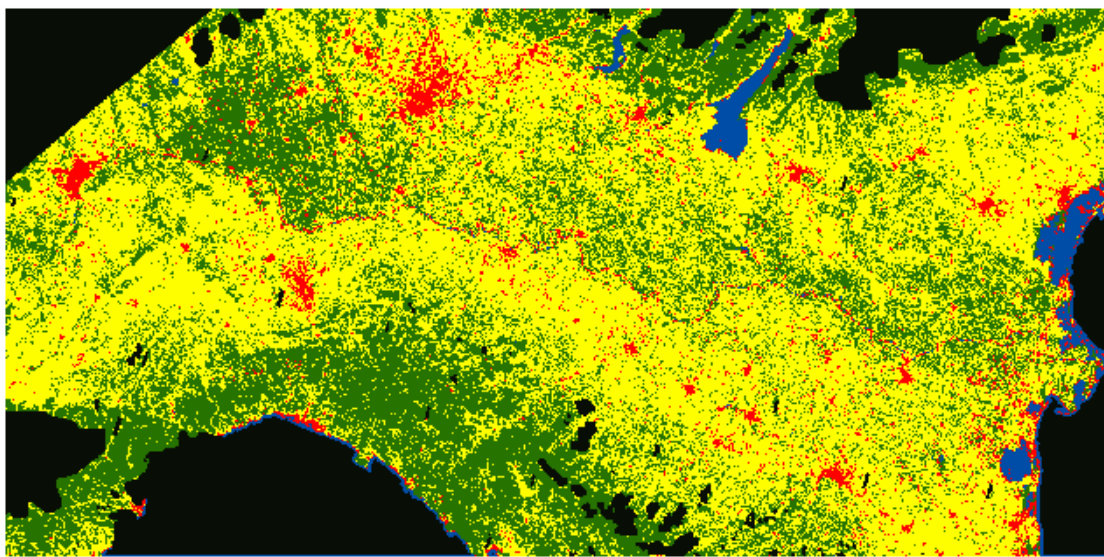


Figure 5 Classification image MODIS 2000 single-date (June) dataset using Maximum Likelihood classification algorithm

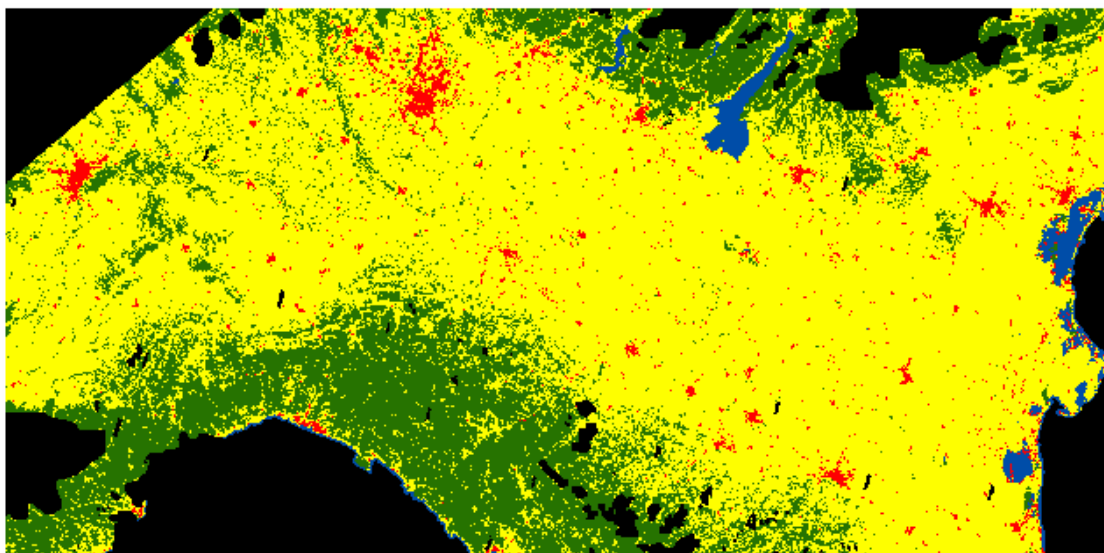


Figure 6 Classification image MODIS 2000 multitemporal dataset using Maximum Likelihood classification algorithm

Table 8 Confusion matrix MODIS 2000 single-date (June) using Maximum Likelihood classification algorithm versus CLC2000 ‘ground truth’

| Overall Accuracy = (924414/1247395) = 74.1076% | | | | | | |
|--|--------------|-------------|--------------|---------|--------|---------|
| Kappa Coefficient = 0.5933 | | | | | | |
| Ground Truth (Pixels) | | | | | | |
| Class | UNCLASSIFIED | 1ARTIFICIAL | 2AGRICULTURE | 3FOREST | 4WATER | Total |
| Unclassified | 194272 | 0 | 0 | 0 | 0 | 194272 |
| 1Artificial | 1 | 23470 | 18648 | 3202 | 4032 | 49353 |
| 2Agriculture | 11 | 52382 | 506338 | 65769 | 2850 | 627350 |
| 3Forest | 3 | 3812 | 167200 | 179839 | 2865 | 353719 |
| 4Water | 619 | 373 | 705 | 509 | 20495 | 22701 |
| Total | 194906 | 80037 | 692891 | 249319 | 30242 | 1247395 |

| Ground Truth (Percent) | | | | | | |
|------------------------|--------------|-------------|--------------|---------|--------|-------|
| Class | UNCLASSIFIED | 1ARTIFICIAL | 2AGRICULTURE | 3FOREST | 4WATER | Total |
| Unclassified | 99.67 | 0 | 0 | 0 | 0 | 15.57 |
| 1Artificial | 0 | 29.32 | 2.69 | 1.28 | 13.33 | 3.96 |
| 2Agriculture | 0.01 | 65.45 | 73.08 | 26.38 | 9.42 | 50.29 |
| 3Forest | 0 | 4.76 | 24.13 | 72.13 | 9.47 | 28.36 |
| 4Water | 0.32 | 0.47 | 0.1 | 0.2 | 67.77 | 1.82 |
| Total | 100 | 100 | 100 | 100 | 100 | 100 |

| Class | Commission (Percent) | Omission (Percent) | Commission (Pixels) | Omission (Pixels) | | |
|--------------|-------------------------|-----------------------|------------------------|----------------------|--|--|
| Unclassified | 0 | 0.33 | 0/194272 | 634/194906 | | |
| 1Artificial | 52.44 | 70.68 | 25883/49353 | 56567/80037 | | |
| 2Agriculture | 19.29 | 26.92 | 121012/627350 | 186553/692891 | | |
| 3Forest | 49.16 | 27.87 | 173880/353719 | 69480/249319 | | |
| 4Water | 9.72 | 32.23 | 2206/22701 | 9747/30242 | | |

| Class | Prod. Acc. | User Acc. | Prod. Acc. | User Acc. | | |
|--------------|------------|-----------|---------------|---------------|--|--|
| | (Percent) | (Percent) | (Pixels) | (Pixels) | | |
| Unclassified | 99.67 | 100 | 194272/194906 | 194272/194272 | | |
| 1Artificial | 29.32 | 47.56 | 23470/80037 | 23470/49353 | | |
| 2Agriculture | 73.08 | 80.71 | 506338/692891 | 506338/627350 | | |
| 3Forest | 72.13 | 50.84 | 179839/249319 | 179839/353719 | | |
| 4Water | 67.77 | 90.28 | 20495/30242 | 20495/22701 | | |

Table 9 Confusion matrix MODIS 2000 multitemporal using Maximum Likelihood classification algorithm versus CLC2000 ‘ground truth’

| Overall Accuracy = (1053280/1247395) = 84.44% | | | | | | |
|---|--------------|-------------|--------------|---------|--------|---------|
| Kappa Coefficient = 0.7402 | | | | | | |
| Ground Truth (Pixels) | | | | | | |
| Class | UNCLASSIFIED | 1ARTIFICIAL | 2AGRICULTURE | 3FOREST | 4WATER | Total |
| Unclassified | 194272 | 0 | 0 | 0 | 0 | 194272 |
| 1Artificial | 351 | 20327 | 6204 | 1426 | 2590 | 30898 |
| 2Agriculture | 17 | 57190 | 629863 | 56802 | 6195 | 750067 |
| 3Forest | 5 | 2346 | 56677 | 190960 | 3599 | 253587 |
| 4Water | 261 | 174 | 147 | 131 | 17858 | 18571 |
| Total | 194906 | 80037 | 692891 | 249319 | 30242 | 1247395 |

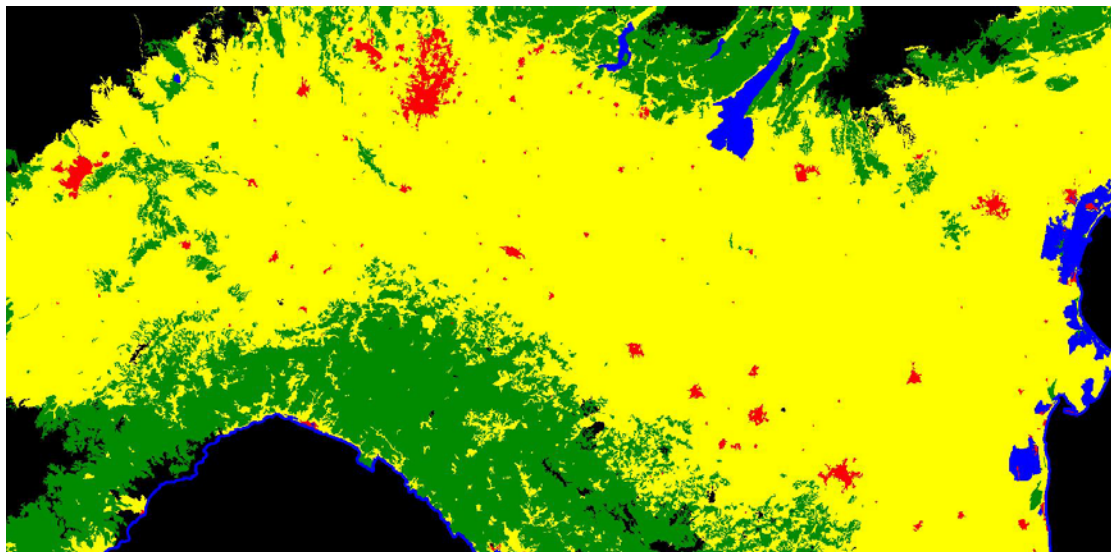
| Ground Truth (Percent) | | | | | | |
|------------------------|--------------|-------------|--------------|---------|--------|-------|
| Class | UNCLASSIFIED | 1ARTIFICIAL | 2AGRICULTURE | 3FOREST | 4WATER | Total |
| Unclassified | 99.67 | 0 | 0 | 0 | 0 | 15.57 |
| 1Artificial | 0.18 | 25.4 | 0.9 | 0.57 | 8.56 | 2.48 |
| 2Agriculture | 0.01 | 71.45 | 90.9 | 22.78 | 20.48 | 60.13 |
| 3Forest | 0 | 2.93 | 8.18 | 76.59 | 11.9 | 20.33 |
| 4Water | 0.13 | 0.22 | 0.02 | 0.05 | 59.05 | 1.49 |
| Total | 100 | 100 | 100 | 100 | 100 | 100 |

| Class | Commission (Percent) | Omission (Percent) | Commission (Pixels) | Omission (Pixels) | | |
|--------------|-------------------------|-----------------------|------------------------|----------------------|--|--|
| Unclassified | 0 | 0.33 | 0/194272 | 634/194906 | | |
| 1Artificial | 34.21 | 74.6 | 10571/30898 | 59710/80037 | | |
| 2Agriculture | 16.03 | 9.1 | 120204/750067 | 63028/692891 | | |
| 3Forest | 24.7 | 23.41 | 62627/253587 | 58359/249319 | | |
| 4Water | 3.84 | 40.95 | 713/18571 | 12384/30242 | | |

| Class | Prod. Acc. (Percent) | User Acc. (Percent) | Prod. Acc. (Pixels) | User Acc. (Pixels) | | |
|--------------|-------------------------|------------------------|------------------------|-----------------------|--|--|
| Unclassified | 99.67 | 100 | 194272/194906 | 194272/194272 | | |
| 1Artificial | 25.4 | 65.79 | 20327/80037 | 20327/30898 | | |
| 2Agriculture | 90.9 | 83.97 | 629863/692891 | 629863/750067 | | |
| 3Forest | 76.59 | 75.3 | 190960/249319 | 190960/253587 | | |
| 4Water | 59.05 | 96.16 | 17858/30242 | 17858/18571 | | |

4.2.2.2. Validation of object-wise result

As predictable, the land cover classification for which the unit of analysis has been ‘upgraded’ from the pixel to CORINE’s object level showed generally higher accuracies compared to the original pixel-based result. A close look to the confusion matrix in Table 10 reveals an overall accuracies of 87.88%, about 4 percentage points higher than for the original pixel based classification. A kappa coefficient of 0.796 confirms a high degree of agreement between this classification and the reference dataset including the off-diagonal values in the calculation. When looking at the class specific figures it is observable how very high accuracies are obtained from the user as well as from the producer stand point for the two vegetation classes and for the water class. Accuracies for these classes range from 73 to 97 percentage points. On the other hand figures for the urban class reflect once more its exceptionality; for this class the confusion matrix reveals a very high user accuracy (97.32%), resulting in almost no commission error and a very low producer accuracy (18.37%) underlying the significance of the omission error. These outcomes can be explained if we consider that the urban class is among all land cover categories the one characterized by smaller and typically scattered objects. In view of this, when applying the majority rule based on CORINE’s polygons, urban pixels are more likely to be lost prompting an underestimation of urban areas in the study region (see Figure 7). In summary, when comparing the pixel- with the object-wise result, for the latter one an overall decrease of the salt-and-pepper effects and the creation of more homogeneous land cover segments are observable. This development is considered positive as the salt-and-pepper effect is generally to be attributed to noise rather than to real land cover distribution patterns. Nevertheless, not all classes seem to benefit equally from the thematic aggregation. For land cover categories such as agriculture, forest and water an improvement in the agreement with CORINE’s map is observed. Regrettably, the divergence becomes larger in the case of the urban class; the percentage of pixels being correctly identified descending from 25.40 to 18.37 when going from the pixel-level to the object-level classification.



Classification Legend

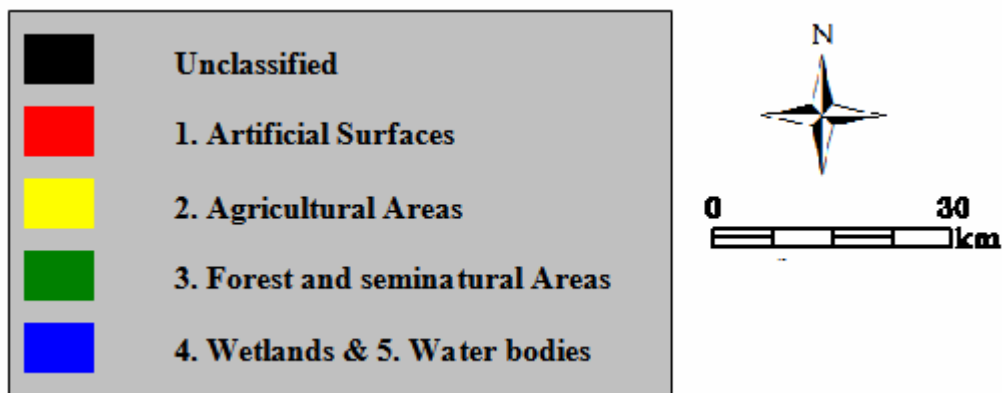


Figure 7 Classification image MODIS 2000 multitemporal dataset resampled to CORINE's polygon level by means of zonal majority rule

Table 10 Confusion matrix ‘object-based’ MODIS 2000 multitemporal classification versus CLC2000 ‘ground truth’

| Overall Accuracy = (1096269/1247395)= 87.8847% | | | | | | |
|---|------------------------------|--------------------|---------------------|----------------|---------------|--------------|
| Kappa Coefficient = 0.796 | | | | | | |
| Class | Ground Truth (Pixels) | | | | | |
| | UNCLASSIFIED | 1ARTIFICIAL | 2AGRICULTURE | 3FOREST | 4WATER | Total |
| Unclassified | 203690 | 0 | 0 | 0 | 0 | 203690 |
| 1Artificial | 0 | 14672 | 135 | 108 | 161 | 15076 |
| 2Agriculture | 0 | 64388 | 654814 | 40552 | 7291 | 767045 |
| 3Forest | 0 | 703 | 36616 | 201049 | 668 | 239036 |
| 4Water | 0 | 123 | 182 | 199 | 22044 | 22548 |
| Total | 203690 | 79886 | 691747 | 241908 | 30164 | 1247395 |

| Ground Truth (Percent) | | | | | | |
|-------------------------------|---------------------|--------------------|---------------------|----------------|---------------|--------------|
| Class | UNCLASSIFIED | 1ARTIFICIAL | 2AGRICULTURE | 3FOREST | 4WATER | Total |
| Unclassified | 100 | 0 | 0 | 0 | 0 | 16.33 |
| 1Artificial | 0 | 18.37 | 0.02 | 0.04 | 0.53 | 1.21 |
| 2Agriculture | 0 | 80.6 | 94.66 | 16.76 | 24.17 | 61.49 |
| 3Forest | 0 | 0.88 | 5.29 | 83.11 | 2.21 | 19.16 |
| 4Water | 0 | 0.15 | 0.03 | 0.08 | 73.08 | 1.81 |
| Total | 100 | 100 | 100 | 100 | 100 | 100 |

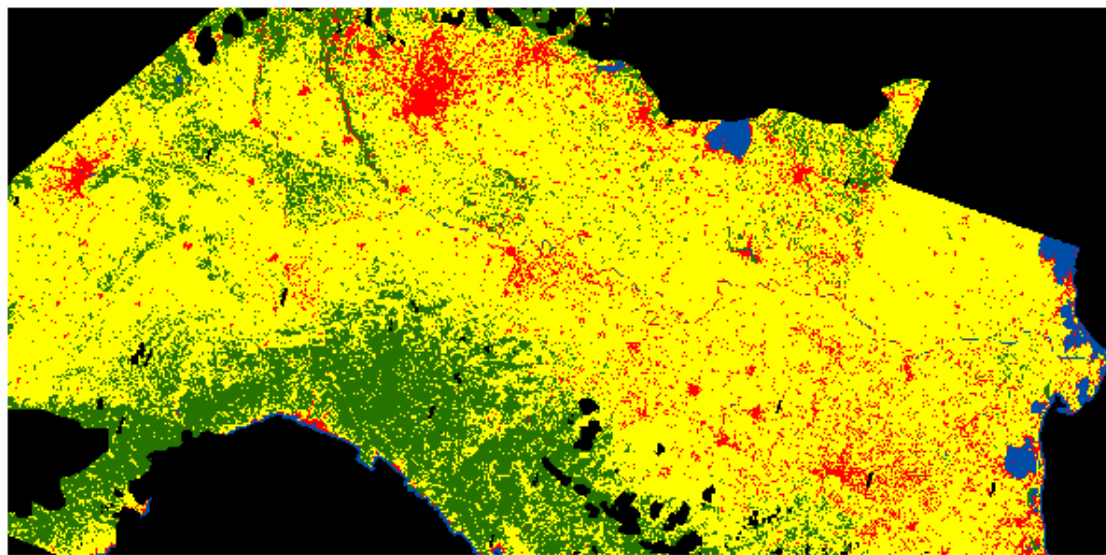
| Class | Commission | Omission | Commission | Omission | | |
|---------------------|-------------------|------------------|-------------------|-----------------|--|--|
| | (Percent) | (Percent) | (Pixels) | (Pixels) | | |
| Unclassified | 0 | 0 | 0/203690 | 0/203690 | | |
| 1Artificial | 2.68 | 81.63 | 404/15076 | 65214/79886 | | |
| 2Agriculture | 14.63 | 5.34 | 112231/767045 | 36933/691747 | | |
| 3Forest | 15.89 | 16.89 | 37987/239036 | 40859/241908 | | |
| 4Water | 2.24 | 26.92 | 504/22548 | 8120/30164 | | |

| Class | Prod. Acc. | User Acc. | Prod. Acc. | User Acc. | | |
|--------------|------------|-----------|---------------|---------------|--|--|
| | (Percent) | (Percent) | (Pixels) | (Pixels) | | |
| Unclassified | 100 | 100 | 203690/203690 | 203690/203690 | | |
| 1Artificial | 18.37 | 97.32 | 14672/79886 | 14672/15076 | | |
| 2Agriculture | 94.66 | 85.37 | 654814/691747 | 654814/767045 | | |
| 3Forest | 83.11 | 84.11 | 201049/241908 | 201049/239036 | | |
| 4Water | 73.08 | 97.76 | 22044/30164 | 22044/22548 | | |

4.2.3. Supervised Classification MODIS 1990

A visual analysis of the MODIS 1990 simulated classification of Figure 8 reveals that scenes have been classified independently from one another, evident from the border lines recognizable when passing from one scene to the other. This unavoidable detail can certainly be identified as the main weaknesses of this thematic product. Nevertheless looking at Table 11, the accuracy assessment based on the CLC1990 dataset identifies this as being the best classification product in the present material, with a 95.39% overall accuracy and a kappa coefficient equal to 0.868. The negative note which once again characterizes also this classification results is the accuracy reached for the urban class, which from the producer point of view is of 45.58% whereas from the user point of view of 41.49%. Commission and omission errors for this class are of the same magnitude underlying the fact that a bit more than half of the pixels are mis-classified (wrongly committed 58.51%, wrongly omitted 54.42%). Generally, the considerations drawn in section 4.2.2., for the MODIS 2000 classification, do apply to the 1990 classification as well and thus will not be repeated at this stage.

What has to be emphasized here is the fact that an overall better performance of the classification algorithm is observed for the 1990 classification. The fact that the classified area for 1990 is of slightly smaller extent (due to Landsat scene coverage) is not believed to be at the origin of this difference. Instead, the question resurfaces on how accurate the MODIS 1990 simulation has been, giving rise to the hypothesis that the resulting product still closely resembles a Landsat dataset. Considering the fact that, although the same classification strategy has been adopted, the 1990 classification gave far better results compared to the 2000 classification ($K_{1990} = 0.868$, $K_{2000} = 0.593$) this does not seam a very remote possibility. What is hypothesized is that the chosen simulation technique missed to model some aspects which differentiate Landsat and MODIS recording and that those aspects are at the origin of the different classifier performance. Moreover, the different pre-processing data have been undergoing prior to distribution is believed to have introduced additional discrepancies. However, no explanation for this difference is evident, and there remains a need for further investigation.



Classification Legend

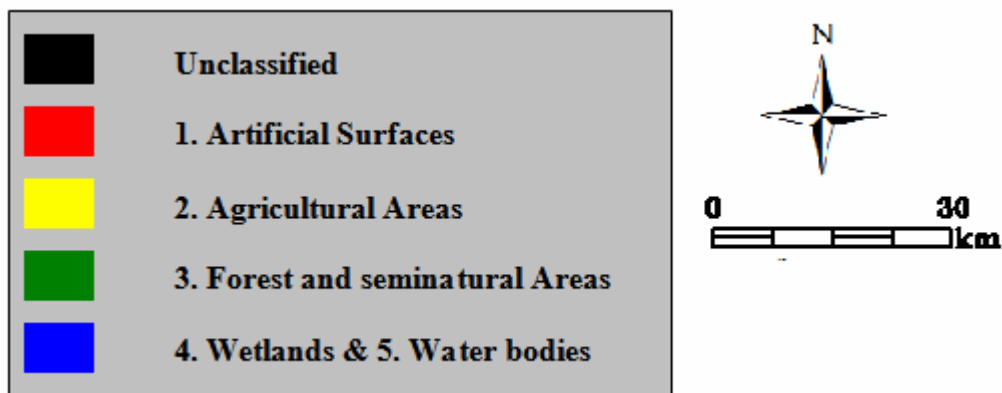


Figure 8 Classification image MODIS 1990 simulated dataset using Maximum Likelihood classification algorithm

Table 11 Confusion matrix MODIS 1990 simulated using Maximum Likelihood classification algorithm versus CLC1990 ‘ground truth’

| Ground Truth (Pixels) | | | | | | |
|-----------------------|--------------|-------------|---------------|---------|--------|---------|
| Class | UNCLASSIFIED | 1ARTIFICIAL | 2AGRICULTURAL | 3FOREST | 4WATER | Total |
| Unclassified | 3730790 | 0 | 0 | 0 | 0 | 3730790 |
| 1Artificial | 0 | 29871 | 34890 | 4160 | 3073 | 71994 |
| 2Agriculture | 0 | 33459 | 555003 | 88596 | 5931 | 682989 |
| 3Forest | 0 | 1866 | 42583 | 161088 | 1139 | 206676 |
| 4Water | 0 | 345 | 493 | 448 | 14969 | 16255 |
| Total | 3730790 | 65541 | 632969 | 254292 | 25112 | 4708704 |

| Ground Truth (Percent) | | | | | | |
|------------------------|--------------|-------------|---------------|---------|--------|-------|
| Class | UNCLASSIFIED | 1ARTIFICIAL | 2AGRICULTURAL | 3FOREST | 4WATER | Total |
| Unclassified | 100 | 0 | 0 | 0 | 0 | 79.23 |
| 1Artificial | 0 | 45.58 | 5.51 | 1.64 | 12.24 | 1.53 |
| 2Agriculture | 0 | 51.05 | 87.68 | 34.84 | 23.62 | 14.5 |
| 3Forest | 0 | 2.85 | 6.73 | 63.35 | 4.54 | 4.39 |
| 4Water | 0 | 0.53 | 0.08 | 0.18 | 59.61 | 0.35 |
| Total | 100 | 100 | 100 | 100 | 100 | 100 |

| Class | Commission | Omission | Commission | Omission | | |
|--------------|------------|-----------|---------------|--------------|--|--|
| | (Percent) | (Percent) | (Pixels) | (Pixels) | | |
| Unclassified | 0 | 0 | 0/3730790 | 0/3730790 | | |
| 1Artificial | 58.51 | 54.42 | 42123/71994 | 35670/65541 | | |
| 2Agriculture | 18.74 | 12.32 | 127986/682989 | 77966/632969 | | |
| 3Forest | 22.06 | 36.65 | 45588/206676 | 93204/254292 | | |
| 4Water | 7.91 | 40.39 | 1286/16255 | 10143/25112 | | |

| Class | Prod. Acc. | User Acc. | Prod. Acc. | User Acc. | | |
|--------------|------------|-----------|-----------------|-----------------|--|--|
| | (Percent) | (Percent) | (Pixels) | (Pixels) | | |
| Unclassified | 100 | 100 | 3730790/3730790 | 3730790/3730790 | | |
| 1Artificial | 45.58 | 41.49 | 29871/65541 | 29871/71994 | | |
| 2Agriculture | 87.68 | 81.26 | 555003/632969 | 555003/682989 | | |
| 3Forest | 63.35 | 77.94 | 161088/254292 | 161088/206676 | | |
| 4Water | 59.61 | 92.09 | 14969/25112 | 14969/16255 | | |

4.3. Change Detection

In this chapter the results of the change detection will be discussed based on the change reports which can be found in Table 12 and Table 13. The two change detection procedures respectively based on the simulated MODIS 1990 image and the CORINE 1990 database as time one data are discussed separately for clarity reasons, although we will see that they reflect similar conclusions. It should be remembered that for the proposed study a post-classification change detection techniques has been chosen, therefore any outcome at this stage has to be seen in the wake of the considerations drawn from the classification results.

4.3.1. Time one image: simulated MODIS 1990 classification

In the following we discuss the change detection as performed from the simulated MODIS 1990 classification image to the June MODIS 2000 classification image. Taking a closer look at the change report figures in Table 12, we can see how from the pixels initially labelled as urban only 31.13% maintained their class label in the Final State image, whereas 59.45% apparently changed into agriculture. This result underlines a decrease of the urban land cover in the study area which is quantified by an Image Difference value of -36.52% obtained via equation (6) (RSI-ENVI, 2006).

$$\frac{(FinalSTATE - InitialSTATE)}{InitialSTATE} * 100 = \frac{(45260 - 71294)}{71294} * 100 = -36.516 \quad (6)$$

The hereby proposed scenario of a recession of the urban class in the study area can certainly be termed erroneous based on prior knowledge about the site and on recognized development trends for the urban class in general. Having acknowledged this, it becomes interesting for this study and for further research to understand the causes behind such an output.

Justifications can be found by linking the abovementioned change figures with the classification results. The confusion matrix presented in Table 11 for the 1990 classification sees about 45.58% of pixel correctly labelled as urban. On the other

hand, when looking at the 2000 classification matrix for the single-date image (Table 8) only 29.32% of the urban pixels have been recognized by the classifier. Consequently, the already high omission error observed for the urban class in the 1990 classification (54.42%) increases even more in the 2000 classification rising up to 70.68%. It follows that, when performing change detection the result can not show anything else than a loss in urban area. The ‘Class Changes’ value of 68.87% for the urban class once more confirms the responsibility of the classification procedures in misleading the change detection outcome.

Table 12 Change Report for unitemporal approach (time one image: simulated MODIS 1990 classification; time two image: original MODIS 2000 classification)

| Pixel Counts | | | | | | |
|-------------------------|-------------|--------------|----------|--------|-----------|-------------|
| | 1Artificial | 2Agriculture | 3Forest | 4Water | Row Total | Class Total |
| Unclassified | 0 | 0 | 0 | 0 | 0 | 322504 |
| 1Artificial | 22192 | 20263 | 1019 | 1786 | 45260 | 45260 |
| 2Agriculture | 42383 | 476338 | 40580 | 648 | 559949 | 559949 |
| 3Forest | 5742 | 163824 | 135172 | 696 | 305434 | 305434 |
| 4Water | 977 | 666 | 146 | 12459 | 14248 | 14248 |
| Class Total | 71294 | 661091 | 176917 | 15589 | 0 | 0 |
| Class Changes | 49102 | 184753 | 41745 | 3130 | 0 | 0 |
| Image Difference | -26034 | -101142 | 128517 | -1341 | 0 | 0 |
| Percentages | | | | | | |
| | 1Artificial | 2Agriculture | 3Forest | 4Water | Row Total | Class Total |
| Unclassified | 0 | 0 | 0 | 0 | 0 | 100 |
| 1Artificial | 31.127 | 3.065 | 0.576 | 11.457 | 100 | 100 |
| 2Agriculture | 59.448 | 72.053 | 22.937 | 4.157 | 100 | 100 |
| 3Forest | 8.054 | 24.781 | 76.404 | 4.465 | 100 | 100 |
| 4Water | 1.37 | 0.101 | 0.083 | 79.922 | 100 | 100 |
| Class Total | 100 | 100 | 100 | 100 | 0 | 0 |
| Class Changes | 68.873 | 27.947 | 23.596 | 20.078 | 0 | 0 |
| Image Difference | -36.516 | -15.299 | 72.643 | -8.602 | 0 | 0 |
| Area (Square Km) | | | | | | |
| | 1Artificial | 2Agriculture | 3Forest | 4Water | Row Total | Class Total |
| Unclassified | 0 | 0 | 0 | 0 | 0 | 20156.5 |
| 1Artificial | 1387 | 1266.44 | 63.69 | 111.63 | 2828.75 | 2828.75 |
| 2Agriculture | 2648.94 | 29771.13 | 2536.25 | 40.5 | 34996.81 | 34996.81 |
| 3Forest | 358.88 | 10239 | 8448.25 | 43.5 | 19089.63 | 19089.63 |
| 4Water | 61.06 | 41.63 | 9.13 | 778.69 | 890.5 | 890.5 |
| Class Total | 4455.88 | 41318.19 | 11057.31 | 974.31 | 0 | 0 |
| Class Changes | 3068.88 | 11547.06 | 2609.06 | 195.63 | 0 | 0 |
| Image Difference | -1627.13 | -6321.38 | 8032.31 | -83.81 | 0 | 0 |

In the attempt to interpret the just reported results a number of considerations come into mind. A decrease in the area of urban land cover successfully recognized by the classifier, was expected as a result of coarsening the resolution (Pax-Lenney and Woodcock, 1997a) and consequently as well a decrease of the change detectable for this class could be anticipated. The loss of information resulting from a ‘coarsening’ of the spatial resolution would not represent a source of concern if interesting equally the 1990 as well as the 2000 MODIS classification. Regrettably, from what reported by the classification accuracy matrixes in Table 11 and Table 8 and by the change report of Table 12 it appears instead to be more pronounced in the time two classification triggering therefore a decrease of the urban class when performing change detection. As emphasized in section 4.2.3. the underlining explanation is believed to be found in the simulation process of the MODIS data for the year 1990.

4.3.2. Time one image: CLC1990 dataset

4.3.2.1. Pixel-wise approach

In the following chapter we discuss the change detection as performed from CLC1990 dataset to the classification image obtained from the MODIS 2000 multitemporal dataset. The change report in Table 13 shows how only 26.69% of the urban pixel preserved their class label whereas 70.18% supposedly changed to agriculture. These results, which apparently worsen compared to the previous case, can again be inferred from the classification outcome of the MODIS 2000 multitemporal dataset (see Table 9) for which only 25.40% of the urban pixel have been correctly identified, making a loss of urban pixels predictable when taking as Initial State classification image the CLC1990 dataset.

Table 13 Change Report for multitemporal approach (date one image: CLC1990 classification; date two image: MODIS 2000 multitemporal classification)

| Pixel Counts | | | | | | |
|---------------------|----------------------|---------------------|---------|--------------------------|-----------|-------------|
| | 1ARTIFICIAL SURFACES | 2AGRICULTURAL AREAS | 3FOREST | 4WATER BODIES & WETLANDS | Row Total | Class Total |
| Unclassified | 0 | 0 | 0 | 0 | 0 | 193428 |
| 1Artificial | 20199 | 6465 | 1418 | 2771 | 30853 | 30853 |
| 2Agriculture | 53124 | 624231 | 64545 | 8603 | 750503 | 750503 |

4. Results and Discussion

| | | | | | | |
|-------------------------|--------|--------|--------|--------|--------|--------|
| 3Forest | 2200 | 50208 | 197525 | 4131 | 254064 | 254064 |
| 4Water | 165 | 120 | 82 | 18180 | 18547 | 18547 |
| Class Total | 75688 | 681024 | 263570 | 33685 | 0 | 0 |
| Class Changes | 55489 | 56793 | 66045 | 15505 | 0 | 0 |
| Image Difference | -44835 | 69479 | -9506 | -15138 | 0 | 0 |

| Percentages | | | | | | |
|-------------------------|----------------------|---------------------|---------|--------------------------|-----------|-------------|
| | 1ARTIFICIAL SURFACES | 2AGRICULTURAL AREAS | 3FOREST | 4WATER BODIES & WETLANDS | Row Total | Class Total |
| Unclassified | 0 | 0 | 0 | 0 | 0 | 100 |
| 1Artificial | 26.687 | 0.949 | 0.538 | 8.226 | 100 | 100 |
| 2Agriculture | 70.188 | 91.661 | 24.489 | 25.54 | 100 | 100 |
| 3Forest | 2.907 | 7.372 | 74.942 | 12.264 | 100 | 100 |
| 4Water | 0.218 | 0.018 | 0.031 | 53.971 | 100 | 100 |
| Class Total | 100 | 100 | 100 | 100 | 0 | 0 |
| Class Changes | 73.313 | 8.339 | 25.058 | 46.029 | 0 | 0 |
| Image Difference | -59.237 | 10.202 | -3.607 | -44.94 | 0 | 0 |

| Area (Square Km) | | | | | | |
|-------------------------|----------------------|---------------------|----------|--------------------------|-----------|-------------|
| | 1ARTIFICIAL SURFACES | 2AGRICULTURAL AREAS | 3FOREST | 4WATER BODIES & WETLANDS | Row Total | Class Total |
| Unclassified | 0 | 0 | 0 | 0 | 0 | 12089.25 |
| 1Artificial | 1262.44 | 404.06 | 88.63 | 173.19 | 1928.31 | 1928.31 |
| 2Agriculture | 3320.25 | 39014.44 | 4034.06 | 537.69 | 46906.44 | 46906.44 |
| 3Forest | 137.5 | 3138 | 12345.31 | 258.19 | 15879 | 15879 |
| 4Water | 10.31 | 7.5 | 5.13 | 1136.25 | 1159.19 | 1159.19 |
| Class Total | 4730.5 | 42564 | 16473.13 | 2105.31 | 0 | 0 |
| Class Changes | 3468.06 | 3549.56 | 4127.81 | 969.06 | 0 | 0 |
| Image Difference | -2802.19 | 4342.44 | -594.13 | -946.13 | 0 | 0 |

Several reasons make it not advisable to directly analyze change in land-cover data based on heterogeneous sources on a pixel-by-pixel basis (Bergen *et al.*, 2005); for the present study in particular six reasons are believed to be determinant. First, the underlying spatial scales of the two datasets were different. The data representing land cover in 1990 were based on CORINE 1990 database, this means data were vector-digitized based on 30m pixel images (Landsat) at 1:100.000 scale and successively aggregated to 250m; on the other hand the MODIS data representing the land cover in 2000 are based on 250m pixels. Additionally, CORINE's dataset has initially been stored in vector format and only in a second step converted to raster format with the typical bias introduced by this process; while MODIS based classification have not undergone any intermediate format conversion. Third, the spectral characteristics of

the two datasets were different. CORINE 1990 dataset was interpreted based on information from the visible (0.45-0.69 μm) and infrared (0.76-0.90, 1.55-1.74, 2.08-2.35 μm) part of the EM spectrum, whereas the MODIS finest spatial resolution product comprises the red band (0.62-0.67 μm) and the near infrared band (0.84-0.88 μm). Third, the original data behind the CORINE and the MODIS classifications have probably undergone different preprocessing (topographic normalization, atmospheric correction, etc.) which has lead to a slightly different information content being elaborated. Fourth, the signal as contained by any given MODIS pixel may actually include some “bleeding” or contamination from adjacent pixels (Bergen *et al.*, 2005), effect that varies significantly with the changing of the pixel size. Moreover, as emphasized in section 3.4.4., spatial mis-registration is expected to occur between the two datasets. Last but not least, the two thematic datasets have been obtained by means of a different methodological approach: while CORINE’s land cover maps have been created by visual interpretation on the object level, MODIS classification is obtained by means of an automatized pixel-based classification approach.

For what concerns the last point, an attempt has been made to narrow the discrepancy between the two datasets by resampling the pixel-based MODIS 2000 classification to CORINE’s polygons level. Results of this approach are presented in the following section.

4.3.2.2. Object-wise approach

The change detection results, obtained using as time 2 image the MODIS 2000 multitemporal classification resampled to CORINE’s object level, are summarized in Table 14.

Table 14 Change Report for multitemporal approach (date one image: CLC1990 classification; date two image: ‘object-based’ MODIS 2000 multitemporal classification)

| Pixel Counts | | | | | | |
|---------------------|-------------|--------------|---------|--------|-----------|-------------|
| | 1Artificial | 2Agriculture | 3Forest | 4Water | Row Total | Class Total |
| Unclassified | 0 | 0 | 0 | 0 | 0 | 179455 |
| 1Artificial | 14651 | 422 | 109 | 164 | 15346 | 15346 |
| 2Agriculture | 60275 | 654916 | 46059 | 9996 | 771246 | 771280 |
| 3Forest | 673 | 27818 | 227779 | 934 | 257204 | 257260 |
| 4Water | 112 | 41 | 61 | 23702 | 23916 | 24054 |

| | | | | | | |
|-------------------------|--------|--------|--------|--------|---|---|
| Class Total | 75711 | 683197 | 274008 | 34796 | 0 | 0 |
| Class Changes | 61060 | 28281 | 46229 | 11094 | 0 | 0 |
| Image Difference | -60365 | 88083 | -16748 | -10742 | 0 | 0 |

| Percentages | | | | | | |
|-------------------------|--------------------|---------------------|----------------|---------------|------------------|--------------------|
| | 1Artificial | 2Agriculture | 3Forest | 4Water | Row Total | Class Total |
| Unclassified | 0 | 0 | 0 | 0 | 0 | 100 |
| 1Artificial | 19.351 | 0.062 | 0.04 | 0.471 | 100 | 100 |
| 2Agriculture | 79.612 | 95.86 | 16.809 | 28.727 | 99.996 | 100 |
| 3Forest | 0.889 | 4.072 | 83.129 | 2.684 | 99.978 | 100 |
| 4Water | 0.148 | 0.006 | 0.022 | 68.117 | 99.426 | 100 |
| Class Total | 100 | 100 | 100 | 100 | 0 | 0 |
| Class Changes | 80.649 | 4.14 | 16.871 | 31.883 | 0 | 0 |
| Image Difference | -79.731 | 12.893 | -6.112 | -30.871 | 0 | 0 |

| Area (Square Km) | | | | | | |
|-------------------------|--------------------|---------------------|----------------|---------------|------------------|--------------------|
| | 1Artificial | 2Agriculture | 3Forest | 4Water | Row Total | Class Total |
| Unclassified | 0 | 0 | 0 | 0 | 0 | 11215.94 |
| 1Artificial | 915.69 | 26.38 | 6.81 | 10.25 | 959.13 | 959.13 |
| 2Agriculture | 3767.19 | 40932.25 | 2878.69 | 624.75 | 48202.88 | 48205 |
| 3Forest | 42.06 | 1738.63 | 14236.19 | 58.38 | 16075.25 | 16078.75 |
| 4Water | 7 | 2.56 | 3.81 | 1481.38 | 1494.75 | 1503.38 |
| Class Total | 4731.94 | 42699.81 | 17125.5 | 2174.75 | 0 | 0 |
| Class Changes | 3816.25 | 1767.56 | 2889.31 | 693.38 | 0 | 0 |
| Image Difference | -3772.81 | 5505.19 | -1046.75 | -671.38 | 0 | 0 |

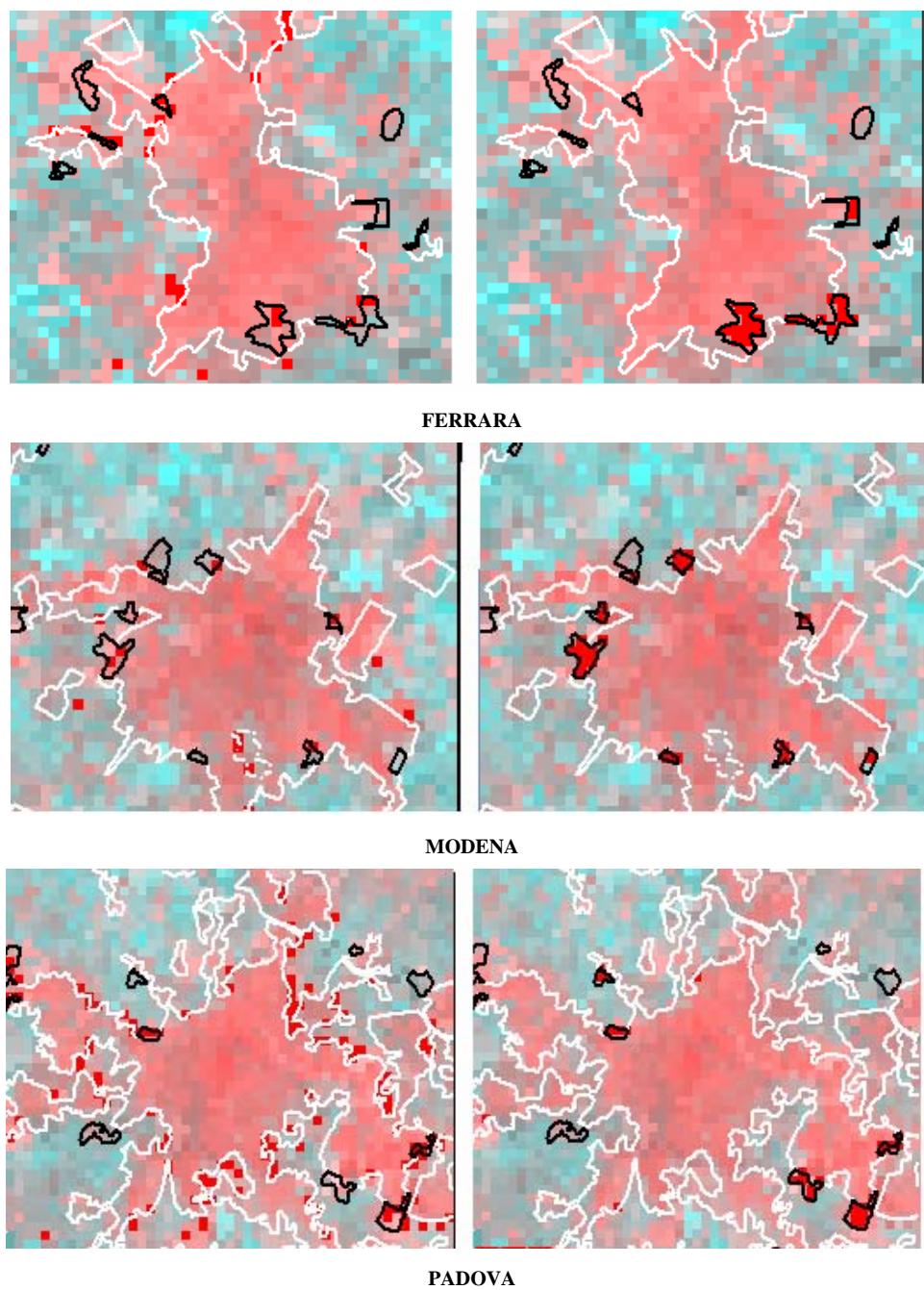
As expected, the visual analysis confirmed that the pixel-wise evaluation is much less favourable and better indications of the detectable changes were obtained by performing a polygon-wise analysis (Figure 10

Figure 10). This is understandable if we consider that, when aggregating to the object level by means of a majority rule, those pixels which mainly represent noise in the signal will be suppressed in the classification. Thus, only real changes and not recording errors or disturbances, are likely to be represented by the change dataset.

A number of visual examples representing a comparison of results between both approaches are presented in the following. The choice of the urban clusters presented is random and only attempted to have a uniformly distributed sample of the major cities located in the study area (Figure 9).



Figure 9 Urban centres, for which a comparison between the pixel- and the object-level change identification, has been performed.



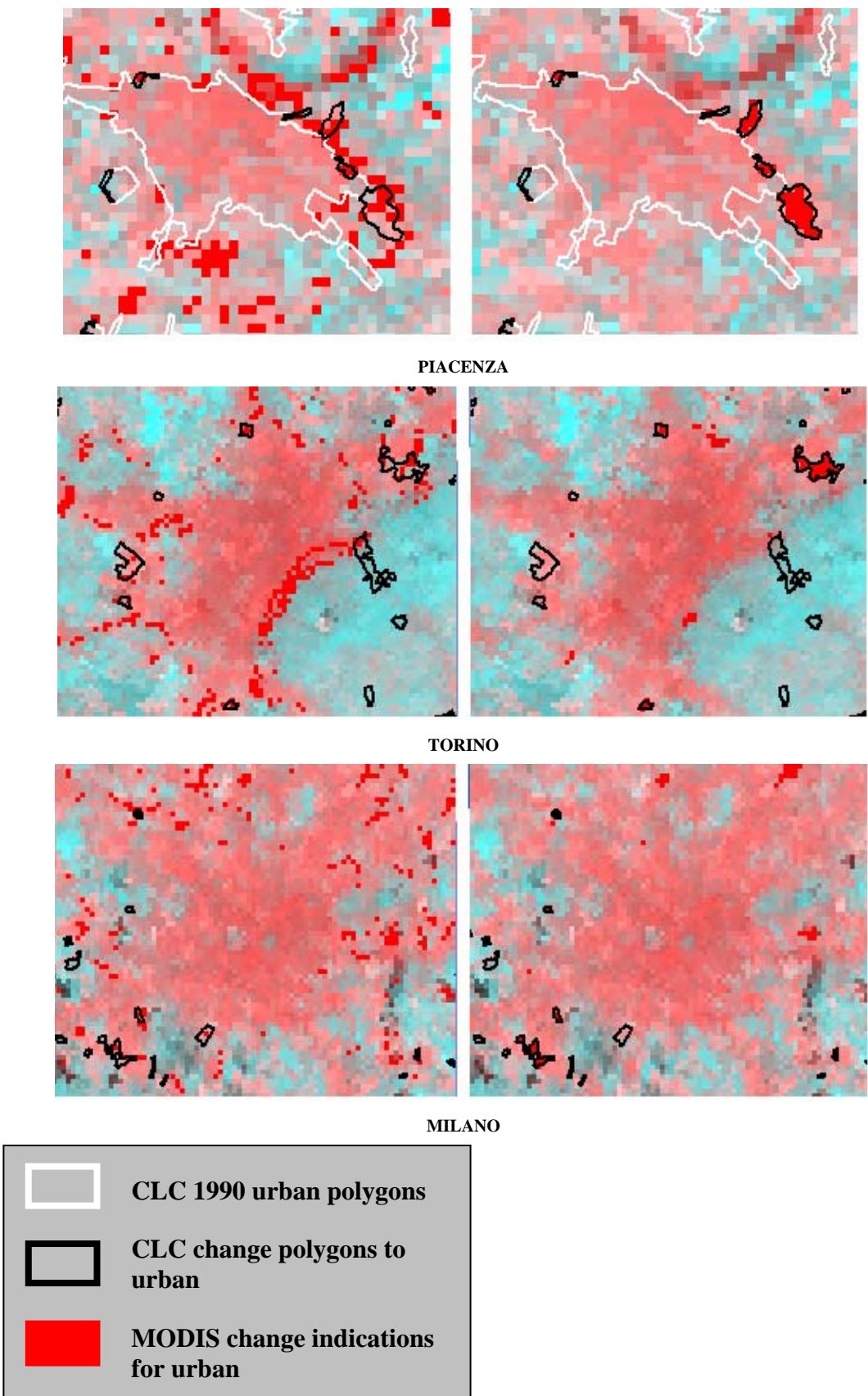


Figure 10 Sample of urban centres located within the study area. Satellite image: MODIS 2000 dataset displayed in red-NIR-NIR layer combination. Left hand side: pixel-level results; Right hand side: object-level results.

5. Conclusions and Recommendations

5.1. Conclusions

The present material provides an approach for land cover mapping and monitoring on the European scale exploiting medium resolution 250m MODIS data. The study further aimed at assessing if such an approach could aid CORINE land cover database update on the first nomenclature level. Particular relevance is there by given to the results obtained for the urban land cover class (“Artificial Surfaces” in CORINE Nomenclature). This is in consideration of the fact that dynamics occurring at the urban scale represent one of the key pressures on biodiversity on which the BIOPRESS initiative concentrates. From the results presented in previous sections of this material, a number of conclusions have been reached which will be reported in the following.

Results revealed the crucial role of spatial resolution, in general for land cover mapping and change detection, and specifically for the urban class. From the classification process, it appeared that the spatial resolution is more critical than the spectral or temporal properties of the data for monitoring of urban land cover. This can be explained with the lack of a clear ‘spectral urban signal’ as already underlined by other authors (Herold *et al.*, 2002a; Herold *et al.*, 2002b) and due to the absence of a seasonal dependency for this class which leads to no-improvement being detected when exploiting a multitemporal dataset. Moreover, it was observed how the coarsening of the resolution generally disfavours especially less represented and fragmented classes leading to their underestimation in the final land cover map as previously observed by Pax-Lenney and Woodcock (1997a).

The fact that some transformations will remain undetected when representing Europe’s fragmented land cover by means of medium resolution data, compared to representation obtainable from the higher resolution solutions, is beyond question. However, it has to be understood that this does not speak against the use of coarser spatial resolutions; it only suggests the necessary assumptions to be made when interpreting the results. First and foremost, the scale at which those data should be used and interpreted has to change. As a result of coarsening spatial resolution, the

operational scale of the resulting thematic map has to adapt to grant consistency with land cover maps derived from higher resolution solutions. Accordingly, also the size and degree of recognizable change will shift to the corresponding scale level. What is more, it is important to note that the so resulting product is not meant to be an areal estimate for land cover change. In other words the change product can not be used as such to quantify the exact amount of change that has occurred in that area it can only be employed to signalize occurrence of land cover transformations.

For the present study the above considerations suggests that the validation against the CORINE datasets should be taken as an indication of disagreement with another land cover map more than as absolute inaccuracies. The risk of drawing wrong conclusions when taking as absolute reference another land cover map originated from different data and classification strategies is suggested by a comparable study conducted by Gallego (2001) in which land cover maps based on higher resolution solutions were compared against CLC datasets.

Having understood this, the disagreement between MODIS based classification results and CLC thematic database is believed merely to underpin the different scale factor and the different methodological approach. We have to remember that CORINE's classification has the object and not the single pixel as unit of analysis, thus reflects the result of an object-oriented approach. When aggregating MODIS pixel-based classification results to CORINE's object level, an improvement of accuracy is observable for all classes besides for urban. Once more the urban class is underestimated due to the size and the scattered organization of its elements which are being suppressed by other classes. Given the fact that a post-classification approach is been adopted, those factors retained responsible for having mislead the comparability of the classification outcome with CLC map, can equally be held responsible for biasing the change analysis.

The answer to the question if medium resolution data hold potential for aiding CORINE's updating process as derived from the present material is twofold. On the one hand, the difficulty of data integration coming from different sources and characterized by different methodological approaches has to be recognized. This material confirmed the inappropriateness of directly analyzing changes in land-cover

data based on heterogeneous sources. On the other hand, MODIS data can very well aid in land cover monitoring without claiming to be able to substitute higher resolution data. The classification results obtained in this study are showing the suitability of MODIS' finest spatial resolution product for mapping CORINE's level 1 Nomenclature classes, with higher accuracies reached for the agricultural and forest categories. Moreover, the obtained change indication could function as a quick and inexpensive means to identify time and locations where significant land cover modification have occurred. MODIS change indication could then serve as an alarm product reflecting the need for a new mapping endeavour based on high resolution data.

Eventually, it can be concluded that the chosen study area can be considered representative for land cover in Europe and therefore similar outcomes are expected in other applications. The exploitation of medium resolution data (particularly MODIS 250m product) for land cover mapping and monitoring on locations characterized by more homogeneous land cover patterns, such as for instance north American landscapes, is expected to be even more successful.

5.2. Recommendations

Based on the indications obtained from the present material we recommend the following to be considered for further research.

This study confirmed that for monitoring at a large scale (regional or global) based on medium to coarse resolution satellite data, land cover changes are normally smaller than or equivalent to the pixel scale and thus misregistration plays a crucial role in their detection and over-/under- estimation. In view of this, methods should be developed and implemented that aim at reducing registration inaccuracies between time one and time two images. A number of authors have already engaged in such an attempt and we refer to their work for further details (Brown, 1992; Stow, 1999; Chalermwat, 1999).

As extensively emphasized in section 5.1., the main source of bias affecting the change detection processes is believed to rely in the lack of a suitable time one image. The lack of MODIS data for the year 1990 has forced us to reach to simulation in one case and to substitution by means of CORINE's land cover 1990 dataset in the other. Regrettably, none of the two options showed itself good enough to replace properly the missing component and thus did not provide with an adequate time one image to use in the change detection process. The time constrain characterizing this study hindered a more sophisticated and thus accurate simulation of the MODIS data for the year 1990; however the pursuing thereof is recommended for further research. First and foremost, to improve the simulation process it is suggested to acquire the original Landsat and MODIS images. Datasets which have been undergoing less possible processing prior to distribution are expected to show a better correlation than has been found in this study.

To compensate partly for the low spectral dimensionality of the 250m MODIS product (only 2 bands) it is recommended to exploit the high temporal frequency with which these data are made available. The fact that for the present study classification results did not improve significantly for the multitemporal approach compared to the single-date one could be related to the fact that only three images, respectively from spring, summer and autumn, were used. The usage of a temporal profile corresponding to an entire MODIS acquisition year should be investigated to improve class discernability.

Last but not least, the introduction in 2002 of a new end-user value-added product of the MODIS series of products, namely the Vegetative Cover Conversion (VCC) product, will stimulate research in land cover monitoring by means of medium resolution data. Nevertheless, further testing is believed to be needed before this product can become fully operational.

Eventually, it is believed that the hereby gained understanding of the methodological and validation requirements for mapping urban areas from medium resolution data will provide a foundation for urban and urban growth mapping in the future. The potential of the MODIS instrument and its suitability for the specific task has here by been partly explored but much work can still be done in this regard.

Bibliography

Alexandridis, T. and Y. Chemin (2002). Landsat ETM+, terra MODIS and NOAA AVHRR:Issues of scale and inter-dependency regarding land parameters. 23rd Asian Conference of Remote Sensing, Kathmandu, Nepal, 25-29th November 2002.

Banko, G. (1998). A review of assessing the accuracy of classifications of remotely sensed data and of methods including remote sensing data in forest inventory, International Institute for Applied Systems Analysis, Luxenburg, Austria: 1-42.

Baulies, X. and G. Szejwach (1998). Survey of needs, gaps and priorities on data for land-use/land-cover change research. LUCC DATA REQUIREMENTS WORKSHOP, Barcelona, Spain, LUCC Report Series No. 3, Institut Cartogràfic de Catalunya.

Ben-Dor, E., N. Levin and H. Saaroni (2001). "A spectral based recognition of the urban environment using the visible and near-infrared spectral region (0.4–1.1 mm). A case study over tel-aviv, israel." International Journal of Remote Sensing 22(11): 2193-2218.

Bergen, K. M., D. G. Brown, J. F. Rutherford and E. J. Gustafson (2005). "Change detection with heterogeneous data using ecoregional stratification, statistical summaries and a land allocation algorithm." Remote Sensing of Environment 97(4): 434-446.

Blaschke, T. (2005). "Towards a framework for change detection based on image objects. Erasmi, s., cyffka, b., kappas, m. (eds.)." Göttingen Geographische Abhandlungen 113: 1-9.

Blaschke, T., S. Lang and M. Moeller (2005). Object-based analysis of remote sensing data for landscape monitoring: Recent developments. Anais XII Simpósio Brasileiro de Sensoriamento Remoto, Goiânia, Brasil, 16-21 april 2005.

Boer, M. E. d., J. D. Vente, C. A. Mücher, W. A. S. Nijenhuis and H. A. M. Thunnissen (2000). Land cover monitoring: An approach towards pan european land cover classification and change detection. bcrs, Alterra: 1-111.

Bossard, M., J. Feranec and J.Otahel (2000). CORINE land cover technical guide - addendum 2000, European Environment Agency: 1-105.

Brown, L. G. (1992). "A survey of image registration techniques." ACM Computing

Surveys 24(4): 325-376.

Chalermwat, P. (1999). High performance automatic image registration for remote sensing. Fairfax, Virginia, George Mason University. PhD thesis: 140.

Chander, G. and B. Markham (2003). "Revised landsat-5 TM radiometric calibration procedures and postcalibration dynamic ranges." IEEE Transactions on Geoscience and Remote Sensing 41(11): 2674-2677

Chavez Jr, P. S. (1988). "An improved dark-object subtraction technique for atmospheric scattering correction of multispectral data." Remote Sensing of Environment 24(3): 459-479.

Cho, S. H. (2000). "Digital change detection by post-classification comparison of multitemporal remotely-sensed data." Journal of the Korean Society of Remote Sensing 16(4): 367-373.

Clark, B. J. F. and P. K. E. Pellikka (2004). The development of a land use change detection methodology for mapping the taita hills, southeast kenya: Radiometric corrections. Proceedings of the 31st International Symposium of Remote Sensing of the Environment, St. Petersburg, Russia, CD-ROM publication.

Clevers, J. G. P. W., H. M. Bartholomeus, C. A. Mücher and A. J. W. D. Wit (2004a). Use of MERIS data for land cover mapping in the Netherlands. MERIS User Workshop, Frascati, Italy, ESA SP-549.

Clevers, J. G. P. W., R. Z. Milla, M. E. Schaepman and H. M. Bartholomeus (2004b). Using MERIS on ENVISAT for land cover mapping. ENVISAT & ERS Symposium, Salzburg, Austria.

Congalton, R. G. (1991). "A review of assessing the accuracy of classifications of remotely sensed data." Remote Sensing of Environment 37(1): 35-46.

Desta, H. S. (2005). Comparison of MODIS and MERIS data for land cover mapping in the netherlands. Geo-information Science. Wageningen, Wageningen University. MSc thesis.

Dwivedi, R. S., S. Kandrika and K. V. Ramana (2004). "Comparison of classifiers of remote-sensing data for land-use/land-cover mapping." Current Science 86(2): 328-335

Edwards, A. J. (1999). Applications of satellite and airborne image data to coastal management. Environment and Development in Coastal Regions and in Small

Islands (CSI): Seventh Computer-based Learning Module. A. J. Edwards. de Fontenoy, Paris, UNESCO: 29.

Foody, G. M. (2001). "Status of land cover classification accuracy assessment." Remote Sensing of Environment 80: 185- 201.

Gallego, F. J. (2001). Comparing CORINE land cover with a more detailed database in arezzo (italy). Towards Agri-environmental indicators: Topic report 6/2001. Copenhagen, European Environment Agency: 118-125.

Giri, C., B. Reed and Z. Zhu (2005). "A comparative analysis of the global land cover 2000 and MODIS land cover data sets." Remote Sensing of Environment 94(1): 123-132.

Hansen, M. C., R. S. DeFries, J. R. G. Townshend, R. Sohlberg, C. Dimiceli and M. Carroll (2002). "Towards an operational MODIS continuous field of percent tree cover algorithm: Examples using AVHRR and MODIS data." Remote Sensing of Environment 83(1-2): 303-319.

Hazeu, G. W. and C. A. Mücher (2005). Historic land use dynamics in and around NATURA2000 sites as indicators for impact on biodiversity - phase I of the BIOPRESS project for the Netherlands. CGI-report 05-001. A.-r. 1077, Centre for Geo-Information: 1-161.

Herold, M., K. C. Clarke and G. Menz (2002a). A multi-scale framework for mapping and analysis of the spatial and temporal pattern of urban growth. 22nd EARSEL Symposium "Geoinformation for European-wide integration, Prague.

Herold, M., M. Gardner, B. Hadley and D. Roberts (2002b). The spectral dimension in urban land cover mapping from high resolution optical remote sensing data. 3rd Symposium on Remote Sensing of Urban Areas, Istanbul, Turkey.

Jonathan, M., M. S. P. Meirelles, J.-P. Berroir and I. Herlin (2005). Regional scale land use/land cover classification using temporal series of modis data. Anais XII Simpósio Brasileiro de Sensoriamento Remoto, Goiânia, Brasil.

Justice, C. O., J. R. G. Townshend, E. F. Vermote, E. Masuoka, R. E. Wolfe, N. Saleous, D. P. Roy and J. T. Morisette (2002). "An overview of MODIS land data processing and product status." Remote Sensing of Environment 83(1-2): 3-15.

Kral, K. (2003). "Review of current and new supervised classification methods of satellite imagery with increased attention to the knowledge base classification (case study: Montagne noir - France)." Ekologia Bratislava 22(SUPPL. 2):

168-181.

Lambin, E. F., B. L. Turner, H. J. Geist, S. B. Agbola and A. Angelsen (2001). "The cause of land-use and land-cover change: Moving beyond the myths." Global Environmental Change 11: 261-269.

Langley, S. K., H. M. Cheshire and K. S. Humes (2001). "A comparison of single date and multitemporal satellite image classifications in a semi-arid grassland." Journal of Arid Environments 49: 401-411.

Lepers, E., E. F. Lambin, A. C. Janetos, R. Defries, F. Achard, N. Ramankutty and R. J. Scholes (2005). "A synthesis of information on rapid land-cover change for the period 1981-2000." BioScience 55 (2): 115-124.

Lillesand, T. M., R. W. Kiefer and J. W. Chipman (2004). Remote sensing and image interpretation. 5th edition, Wiley.

Lu, D., P. Mausel, E. Brondizio and E. Moran (2004). "Change detection techniques." International Journal of Remote Sensing 25(12): 2365-2407.

Lunetta, R. S., D. M. Johnson, J. G. Lyon and J. Crotwell (2004). "Impacts of imagery temporal frequency on land-cover change detection monitoring." Remote Sensing of Environment 89(4): 444-454.

Mas, J. F. (1999). "Monitoring land-cover changes: A comparison of change detection techniques." International Journal of Remote Sensing 20(1): 139 - 152.

Masek, J. G., M. Honzak, S. N. Goward, P. Liu and E. Pak (2001). "Landsat-7 ETM+ as an observatory for land cover initial radiometric and geometric comparisons with Landsat-5 thematic mapper." Remote Sensing of Environment 78(1-2): 118-130.

Moeller, M. S. and T. Blaschke (2005). Monitoring LULC dynamics in the urban - rural fringe. Anais XII Simposio Brasiliense de Sensoriamento Remoto, Goiania, Brasil.

Morissette, J. T., J. L. Privette and C. O. Justice (2002). "A framework for the validation of MODIS land products." Remote Sensing of Environment 83: 77-96.

Mücher, C. A., K. T. Steinnocher, F. P. Kressler and C. Heunks (2000). "Land cover characterization and change detection for environmental monitoring of pan-europe." International Journal of Remote Sensing 21(6&7): 1159-1181.

Pax-Lenney, M. and C. E. Woodcock (1997a). "The effect of spatial resolution on the ability to monitor the status of agricultural lands." Remote Sensing of Environment 61(2): 210-220.

Pax-Lenney, M. and C. E. Woodcock (1997b). "Monitoring agricultural lands in Egypt with multitemporal Landsat TM imagery: How many images are needed?" Remote Sensing of Environment 59(3): 522-529.

Perdigao, V. and A. Annoni (1997). Technical and methodological guide for updating CORINE land cover data base, European Environmental Agency - Joint Research Centre.

Price, J. C. (2003). "Comparing MODIS and ETM+ data for regional and global land classification." Remote Sensing of Environment 86(4): 491-499.

Reid, W. V., H. A. Mooney, A. Cropper, D. Capistrano, S. R. Carpenter, K. Chopra, Partha Dasgupta, Thomas Dietz, Anantha Kumar Duraiappah, Rashid Hassan, Roger Kasperson, Rik Leemans, Robert M. May, Tony (A.J.) McMichael, Prabhu Pingali, Cristián Samper, Robert Scholes, Robert T. Watson, A.H. Zakri, Zhao Shidong, Neville J. Ash, Elena Bennett, Pushpam Kumar, Marcus J. Lee, Ciara Raudsepp-Hearne, Henk Simons, Jillian Thonell and M. B. Zurek (2005). Ecosystems and human well-being. synthesis / Millennium Ecosystem Assessment. J. Sarukhán and A. Whyte. Island Press, Washington, DC., World Resources Institute: 1-155.

Rogan, J. and D. M. Chen (2004). "Remote sensing technology for mapping and monitoring land-cover and land-use change." Progress in Planning 61: 301-325.

RSR (2006). ENVI User's Guide, Research Systems, Inc.

Schneider, A., M. A. Friedl, D. K. McIver and C. E. Woodcock (2003). "Mapping urban areas by fusing multiple sources of coarse resolution remotely sensed data." Photogrammetric Engineering and Remote Sensing 69(12): 1377-1386.

Skinner, L. and A. Luckman (2004). Deriving landcover information over Siberia using MERIS and MODIS data. Proc. MERIS User Workshop, Frascati, Italy.

Song, C., C. E. Woodcock, K. C. Seto, M. P. Lenney and S. A. Macomber (2001). "Classification and change detection using Landsat TM data: When and how to correct atmospheric effects?" Remote Sensing of Environment 75(2): 230-244.

Stefanov, W. L. and M. Netzband (2005). "Assessment of ASTER land cover and MODIS NDVI data at multiple scales for ecological characterization of an arid

urban centre." Remote Sensing of Environment 99(1-2): 31-43.

Stow, D. A. (1999). "Reducing the effects of misregistration on pixel-level change detection." International Journal of Remote Sensing 20(12): 2477- 2483.

Tatem, A. J., A. M. Noor and S. I. Hay (2005). "Assessing the accuracy of satellite derived global and national urban maps in Kenya." Remote Sensing of Environment 96(1): 87-97.

Townshend, J. R. G. and C. O. Justice (1988). "Selecting the spatial resolution of satellite sensors required for global monitoring of land transformations." International Journal of Remote Sensing 9(2): 187-236.

Townshend, J. R. G. and C. O. Justice (2002). "Towards operational monitoring of terrestrial systems by moderate-resolution remote sensing." Remote Sensing of Environment 83(1-2): 351-359.

Tucker, C. J., D. M. Grant and J. D. Dykstra (2004). "NASA's global orthorectified Landsat data set." Photogrammetric Engineering & Remote Sensing 70(3): 313-322.

Vermote, E. F., N. Z. El Saleous and C. O. Justice (2002). "Atmospheric correction of MODIS data in the visible to middle infrared: First results." Remote Sensing of Environment 83(1-2): 97-111.

Walter, V. (2004). "Object-based classification of remote sensing data for change detection." ISPRS Journal of Photogrammetry & Remote Sensing 58: 225-238.

Walter, V. and D. Fritsch (2000). Automated revision of GIS databases. 8th AVM Symposium on GIS, Washington D.C., USA.

Weber, J.L. and G. Hazeu (2004). Subreport 3 Halting biodiversity loss - Section 3.1 Land use changes, submitted for contribution to SOER2005, EEA, 1-10

Woodcock, C. E. and A. H. Strahler (1987). "The factor of scale in remote sensing." Remote Sensing of Environment 21(3): 311-332.

Zhan, X., R. Defries, J. R. G. Townshend, C. Dimiceli, M. Hansen, C. Huang and R. Sohlberg (2000). "The 250m global land cover change product from the moderate resolution imaging spectroradiometer of NASA's earth observing system." International Journal of Remote Sensing 21(6 & 7): 1433-1460.

Zhan, X., R. A. Sohlberg, J. R. G. Townshend, C. DiMiceli, M. L. Carroll, J. C.

Eastman, M. C. Hansen and R. S. DeFries (2002). "Detection of land cover changes using MODIS 250 m data." Remote Sensing of Environment 83(1-2): 336-350.

Websites:

Landsat 7 Science Users Handbook

http://ltpwww.gsfc.nasa.gov/IAS/handbook/handbook_htmls/chapter1/chapter1.html

Global Land Cover Facility

<http://glcfapp.umiacs.umd.edu/index.shtml>

Image 2000 & Corine Land Cover 2000 Project

<http://image2000.jrc.it/>

European Environment Agency data service

<http://dataservice.eea.eu.int/dataservice/>

MODIS Land Global Browse Images

<http://landqa2.nascom.nasa.gov/cgi-bin/browse/browse.cgi>

Earth Observing System Data Gateway

<http://edcimswww.cr.usgs.gov/pub/imswelcome/>

User Guide for MOD44A VCC

<http://glcf.umiacs.umd.edu/data/modis/vcc/>

Legambiente

<http://www.legambiente.com>

Center for Earth Observation (CEO) at Yale University

<http://www.yale.edu/ceo>

BIOPRESS

<http://www.creaf.uab.es/biopress/index2.htm>

Appendix

Appendix 1. MODIS Specifications

| | |
|----------------------------|--|
| Orbit: | 705 km, 10:30 a.m. descending node (Terra) or 1:30 p.m. ascending node (Aqua), sun-synchronous, near-polar, circular |
| Scan Rate: | 20.3 rpm, cross track |
| Swath | 2330 km (cross track) by 10 km (along track at nadir) |
| Dimensions: | |
| Telescope: | 17.78 cm diam. off-axis, afocal (collimated), with intermediate field stop |
| Size: | 1.0 x 1.6 x 1.0 m |
| Weight: | 228.7 kg |
| Power: | 162.5 W (single orbit average) |
| Data Rate: | 10.6 Mbps (peak daytime); 6.1 Mbps (orbital average) |
| Quantization: | 12 bits |
| Spatial Resolution: | 250 m (bands 1-2) 500 m (bands 3-7) 1000 m (bands 8-36) |
| Design Life: | 6 years |

| Primary Use | Band | Bandwidth ¹ | Spectral Radiance ² | Required SNR ³ |
|--|------|------------------------|--------------------------------|---------------------------|
| Land/Cloud/Aerosols Boundaries | 1 | 620 - 670 | 21.8 | 128 |
| | 2 | 841 - 876 | 24.7 | 201 |
| Land/Cloud/Aerosols Properties | 3 | 459 - 479 | 35.3 | 243 |
| | 4 | 545 - 565 | 29.0 | 228 |
| | 5 | 1230 - 1250 | 5.4 | 74 |
| | 6 | 1628 - 1652 | 7.3 | 275 |
| | 7 | 2105 - 2155 | 1.0 | 110 |
| | 8 | 405 - 420 | 44.9 | 880 |
| | 9 | 438 - 448 | 41.9 | 838 |
| Ocean Color/Phytoplankton/Biogeochemistry | 10 | 483 - 493 | 32.1 | 802 |
| | 11 | 526 - 536 | 27.9 | 754 |
| | 12 | 546 - 556 | 21.0 | 750 |
| | 13 | 662 - 672 | 9.5 | 910 |
| | 14 | 673 - 683 | 8.7 | 1087 |
| | 15 | 743 - 753 | 10.2 | 586 |
| | 16 | 862 - 877 | 6.2 | 516 |
| | 17 | 890 - 920 | 10.0 | 167 |
| | 18 | 931 - 941 | 3.6 | 57 |
| Atmospheric Water Vapor | 19 | 915 - 965 | 15.0 | 250 |

| Primary Use | Band | Bandwidth ¹ | Spectral Radiance ² | Required NE[delta]T(K) ⁴ |
|----------------------------------|------|------------------------|--------------------------------|-------------------------------------|
| Surface/Cloud Temperature | 20 | 3.660 - 3.840 | 0.45(300K) | 0.05 |
| | 21 | 3.929 - 3.989 | 2.38(335K) | 2.00 |
| | 22 | 3.929 - 3.989 | 0.67(300K) | 0.07 |
| | 23 | 4.020 - 4.080 | 0.79(300K) | 0.07 |
| Atmospheric Temperature | 24 | 4.433 - 4.498 | 0.17(250K) | 0.25 |
| | 25 | 4.482 - 4.549 | 0.59(275K) | 0.25 |

| | | | | |
|--|----|-----------------|------------|----------|
| Cirrus Clouds Water Vapor | 26 | 1.360 - 1.390 | 6.00 | 150(SNR) |
| | 27 | 6.535 - 6.895 | 1.16(240K) | 0.25 |
| | 28 | 7.175 - 7.475 | 2.18(250K) | 0.25 |
| Cloud Properties | 29 | 8.400 - 8.700 | 9.58(300K) | 0.05 |
| Ozone | 30 | 9.580 - 9.880 | 3.69(250K) | 0.25 |
| Surface/Cloud Temperature | 31 | 10.780 - 11.280 | 9.55(300K) | 0.05 |
| | 32 | 11.770 - 12.270 | 8.94(300K) | 0.05 |
| Cloud Top Altitude | 33 | 13.185 - 13.485 | 4.52(260K) | 0.25 |
| | 34 | 13.485 - 13.785 | 3.76(250K) | 0.25 |
| | 35 | 13.785 - 14.085 | 3.11(240K) | 0.25 |
| | 36 | 14.085 - 14.385 | 2.08(220K) | 0.35 |

¹ Bands 1 to 19 are in nm; Bands 20 to 36 are in μm
² Spectral Radiance values are ($\text{W}/\text{m}^2 \cdot \mu\text{m}\cdot\text{sr}$)
³ SNR = Signal-to-noise ratio
⁴ NE(delta)T = Noise-equivalent temperature difference

Note: Performance goal is 30-40% better than required

Appendix 2. Equation for the conversion of radiance to apparent reflectance and explanation of its input parameters (Landsat 7 Science Data Users Handbook: (http://ltpwww.gsfc.nasa.gov/IAS/handbook/handbook_htmls/chapter11/chapter11.html))

APPARENT REFLECTANCE:

$$\rho_p = \frac{\pi * L_\lambda * d^2}{ESUN_\lambda * \cos\theta_s}$$

EARTH-SUN DISTANCE IN ASTRONOMICAL UNITS:

$$d = (1 - 0.016729 * \cos(0.9856(DOY - 4)))$$

| Scene | Calendar date (dd/mm/yyyy) | Julian date (DOY) |
|------------|----------------------------|-------------------|
| TM 192_029 | 07/08/1991 | 219 |
| TM 193_028 | 16/08/1992 | 229 |
| TM 193_029 | 12/09/1990 | 255 |
| TM 194_028 | 31/08/1989 | 243 |
| TM 194_029 | 04/07/1991 | 185 |

| Scene | Calendar date (dd/mm/yyyy) | Julian date |
|-------------|----------------------------|-------------|
| ETM 192_029 | 20/06/2000 | 172 |
| ETM 193_028 | 13/09/1999 | 172 |
| ETM 193_029 | 01/08/2001 | 213 |
| ETM 194_028 | 21/06/2001 | 172 |
| ETM 194_029 | 22/09/2000 | 266 |

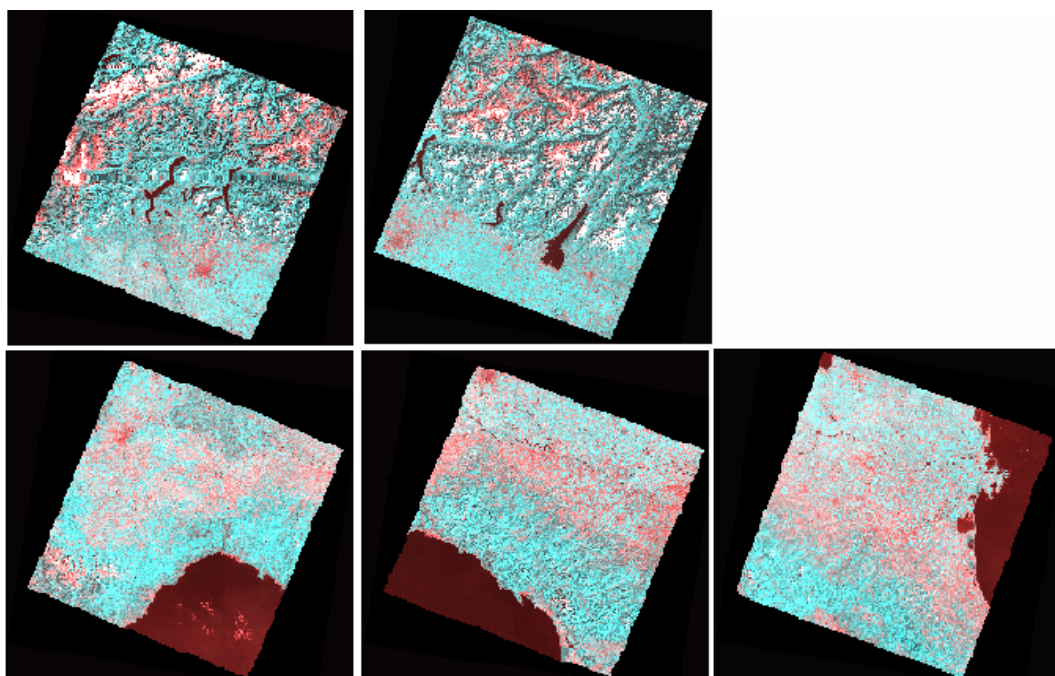
MEAN SOLAR EXOATMOSPHERIC IRRADIANCE:

| Sensor | Band | ESUN (W/m^2*μm) |
|--------|------|-----------------|
| TM | 3 | 1554 |
| | 4 | 1036 |
| ETM+ | 3 | 1551 |
| | 4 | 1044 |

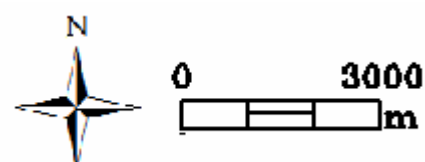
SOLAR ZENITH ANGLE:

$$\Theta = \pi * (90.0 - \text{sun elevation}) / 180.0$$

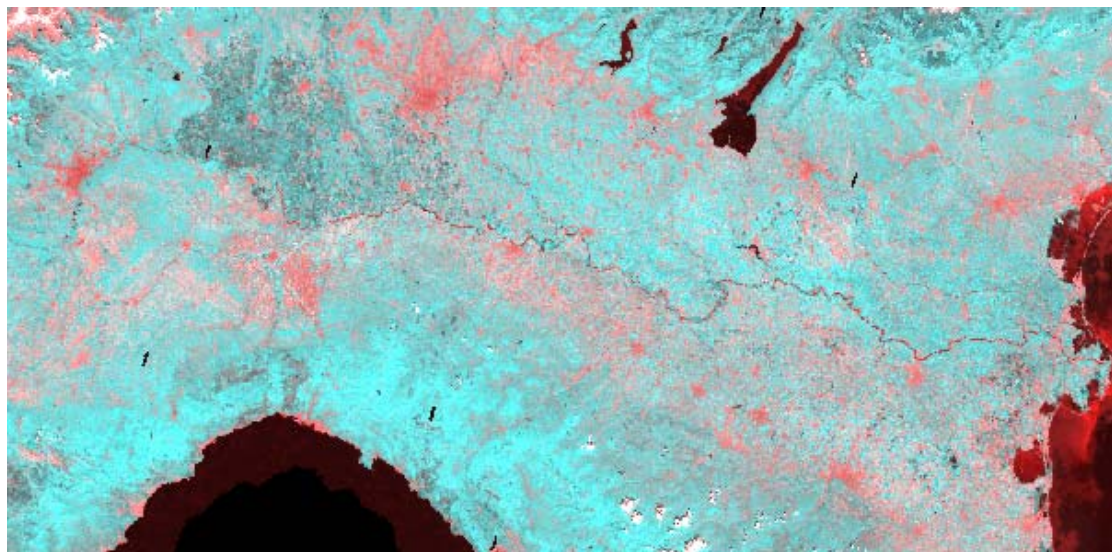
Appendix 3. Landsat TM scenes after preprocessing (from left upper row to right lower row: 194_028, 193_028, 194_029, 193_029, 192_029)



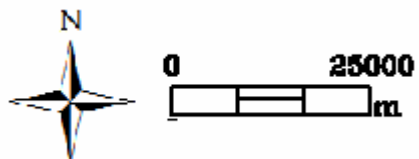
Pixel Size 30 meters
 Projection Albers Conical Equal Area
 Datum WGS 72



Appendix 4. MODIS 2000 June image after preprocessing



Pixel Size 250 meters
Projection Albers Conical Equal Area
Datum WGS 72



Appendix 5. IDL Script used for Landsat's radiometric calibration (created by Allard de Wit in 2000 and adjusted for the purpose of this study)

```

PRO cgi_envi_processor_DN_to_ref
;Select input file (NDVI or something else)
envi_select, title='Select Input Filename', fid=infid, pos=inpos, dims=dims
IF (infid eq -1) THEN RETURN

;Query input file for information (lines, columns, bands, etc)
envi_file_query, infid, data_type=data_type, xstart=xstart,$
  ystart=ystart, interleave=interleave, nb=nb, nl=nl, ns=ns
map_info=          (fid=infid)
proj_info=          (fid=infid)

outfile1=          (filter='*.img', title='Select Output File!')
IF (outfile1 eq '') THEN RETURN
OPENW, unit1, outfile1, /GET_LUN

;Open input files and initialise tiling
interleave=1
tile_id1 =          (infid, inpos, num_tiles=num_tiles, interleave=interleave)

;Initialise reporting
rstr=['Processing:', 'Output to : '+outfile1]
envi_report_init, rstr, title="Processing", base=base, /interrupt
envi_report_inc, base, num_tiles
pi=3.141592654
LMAX=157.400
LMIN=-5.100
gain=(LMAX-LMIN)/255
bias=LMIN
ESUN=1044 ; TM solar exoatmospheric spectral irradiance band specific (from paper)
DOY=256;Day Of the Year following the Julian calendar scene specific (see Excel file)
su=44.67 ; Sun elevation angle from header file scene specific (see Excel file)
d=(1-0.016729*COS(0.9856*(DOY-4))) ; Earth-sun distance in astronomical units (from paper)
theta=pi*(90-su)/180 ; Solar zenith angle in degrees

;Main processing loop
FOR i=0L, num_tiles-1 DO BEGIN
  envi_report_stat,base, i, num_tiles
  data =          (tile_id1, i)
  rad= gain*data + bias
  result = (pi*rad*d^2)/ESUN*COS(theta)
  WRITEU, unit1, result
ENDFOR
envi_report_init, base=base, /finish
envi_tile_done, tile_id1
CLOSE, unit1
FREE_LUN, unit1

data_type = SIZE(result, /TYPE)

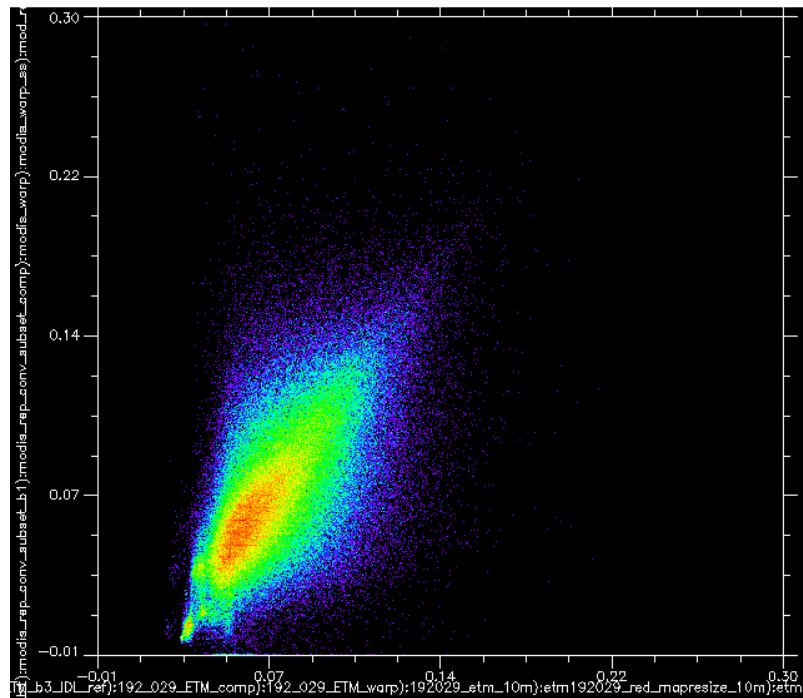
envi_setup_head, fname=outfile1, ns=ns, nl=nl, nb=nb, $
  data_type=data_type, offset=0, interleave=interleave, $
  xstart=xstart+dims[1], ystart=ystart+dims[3], $
  descrip='Image converted to radiance', /write, /open, $
  map_info=map_info
END

```

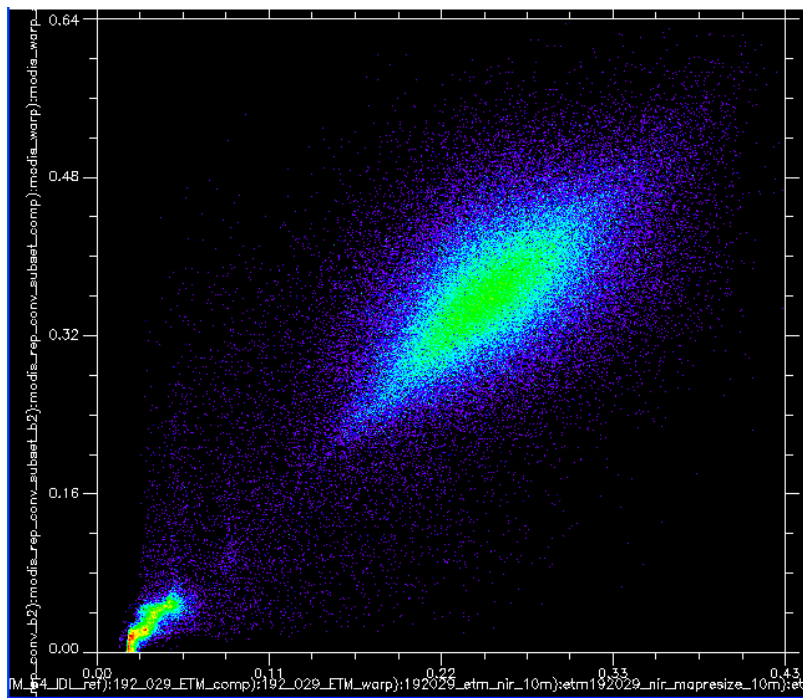
Appendix 6. CORINE Land Cover Nomenclature

| Level 1 | Level 2 | Level 3 |
|----------------------------------|--|---|
| 1. Artificial surfaces | 1.1. Urban fabric 1.2. Industrial, commercial and transport units 1.3. Mines, dumps and construction sites 1.4. Artificial non-agricultural vegetated areas | 1.1.1. Continuous urban fabric 1.1.2. Discontinuous urban fabric 1.2.1. Industrial or commercial units 1.2.2. Road and rail networks and associated land 1.2.3. Sea ports 1.2.4. Airport 1.3.1. Mineral extraction site 1.3.2. Dump 1.3.3. Construction site 1.4.1. Green urban areas 1.4.2. Sport and leisure facilities |
| 2. Agricultural areas | 2.1. Arable land 2.2. Permanent crops 2.3. Pastures 2.4. Heterogeneous agricultural areas | 2.1.1. Non irrigated arable land 2.1.2. Permanently irrigated land 2.1.3. Rice fields 2.2.1. Vineyards 2.2.2. Fruit trees and berries plantations 2.2.3. Olives groves 2.3.1. Pastures 2.4.1. Annual crops associated with permanent crops 2.4.2. Complex cultivation patterns 2.4.3. Land principally occupied by agriculture, with significant areas of natural vegetation 2.4.4. Agro-forestry areas |
| 3. Forest and semi natural areas | 3.1. Forests 3.2. Scrub and/or herbaceous vegetation associations 3.3. Open spaces with little or no vegetation | 3.1.1. Broad leaved-forest 3.1.2. Coniferous forest 3.1.3. Mixed forest 3.2.1. Natural grassland 3.2.2. Moors and heathlands 3.2.3. Sclerophyllous vegetation 3.2.4. Transitional woodland-scrub 3.3.1. Beaches, dunes, sand 3.3.2. Bare rocks 3.3.3. Sparsely vegetated areas 3.3.4. Burnt areas 3.3.5. Glacier and permanent snow-fields |
| 4. Wetlands | 4.1. Inland wetlands 4.2. Coastal wetlands | 4.1.1. Inland marshes 4.1.2. Peat bogs 4.2.1. Salt marshes 4.2.2. Salines 4.2.3. Intertidal flats |
| 5. Water bodies | 5.1. Continental waters 5.2. Marine waters | 5.1.1. Stream courses 5.1.2. Water bodies 5.2.1. Coastal lagoons 5.2.2. Estuaries 5.2.3. Sea and ocean |

Appendix 7. Scatterplot ETM+ (X) plotted against MODIS 2000 (Y).
(A) Red band, (B) Near Infrared band



(A)



(B)